

Supplementary Materials:

New rhenium-tricarbonyl complexes bearing halogen-substituted bidentate ligands: Structural, computational and Hirshfeld surfaces studies

Reza Kia,^{1,*}, Soheil Mahmudi¹ and Paul R. Raithby²

- 1) *Chemistry Department, Sharif University of Technology, P.O. Box 11155-3516, Tehran, Iran*
- 2) *Department of Chemistry, University of Bath, Claverton Down, Bath, BA2 7AY, UK*

* E-mail: rkia@sharif.edu, zsrkk@yahoo.com; Tel.: +98-21-66165332

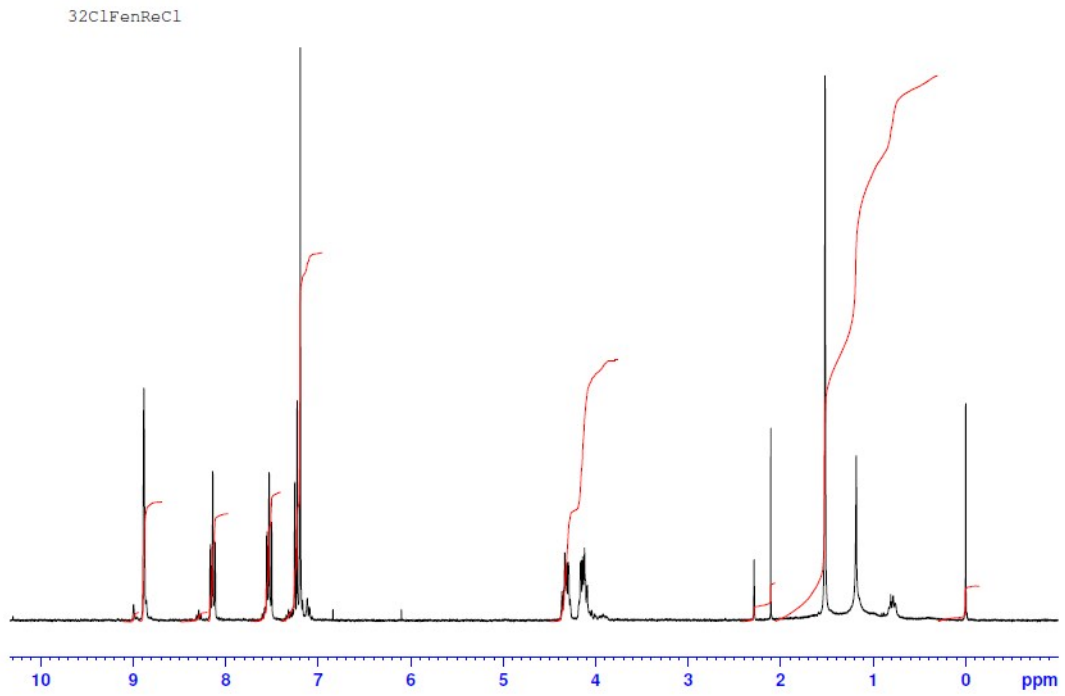


Fig. S1. ¹H-NMR spectrum of **C2** in CDCl₃.

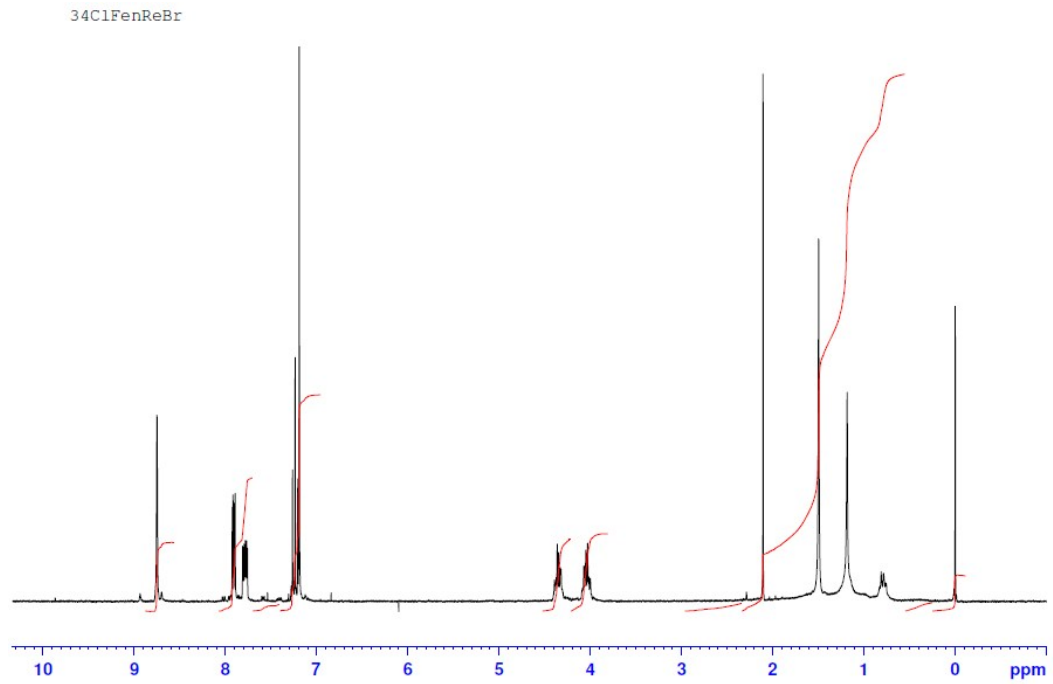


Fig. S2. ¹H-NMR spectrum of **C3** in CDCl₃.

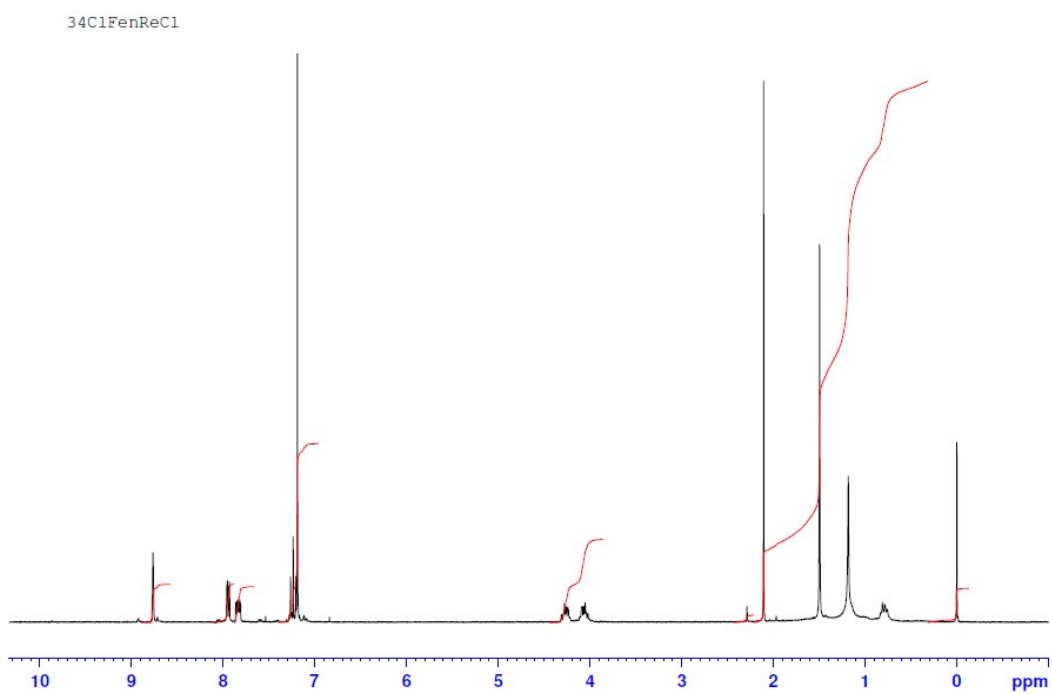


Fig. S3. ¹H-NMR spectrum of **C4** in CDCl₃.

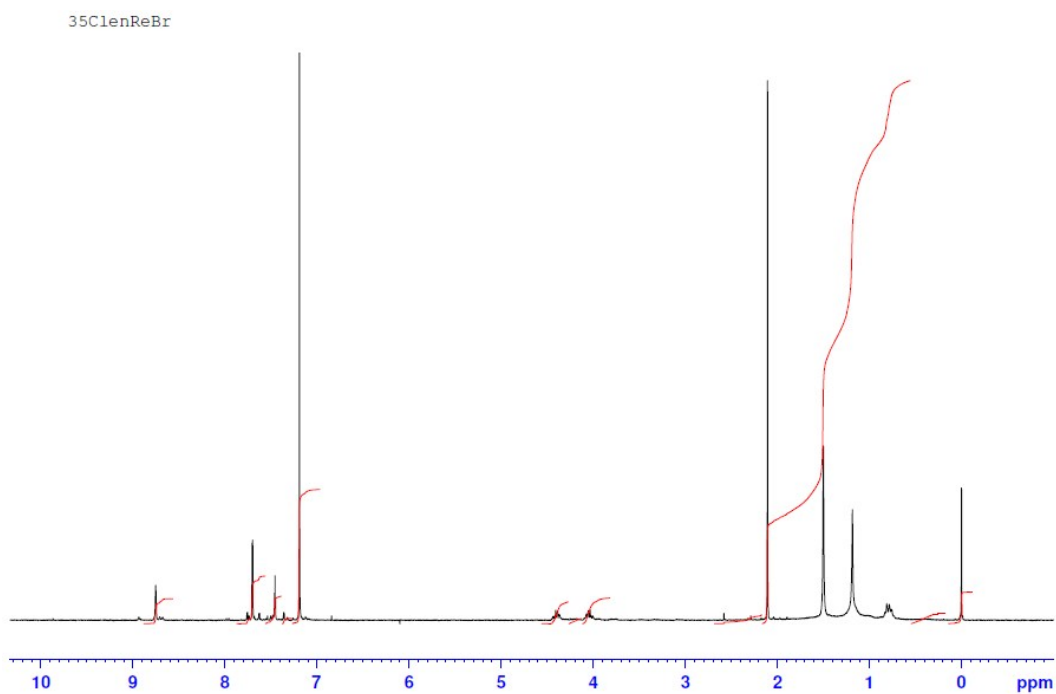


Fig. S4. ¹H-NMR spectrum of **C5** in CDCl₃.

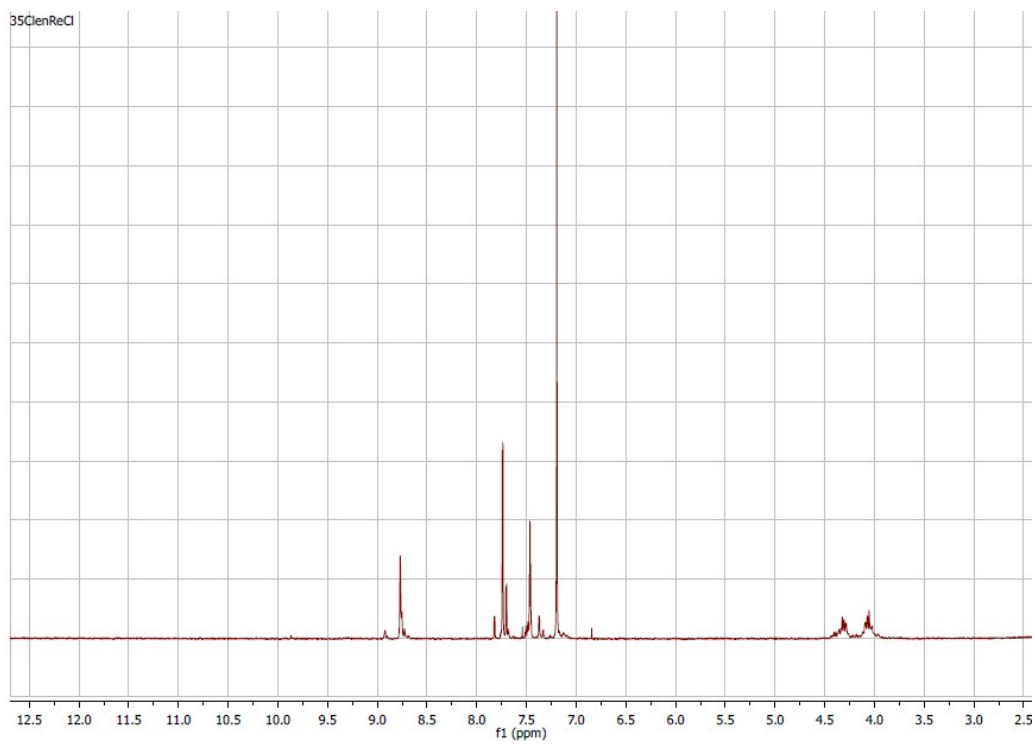


Fig. S5. $^1\text{H-NMR}$ spectrum of **C6** in CDCl_3 .

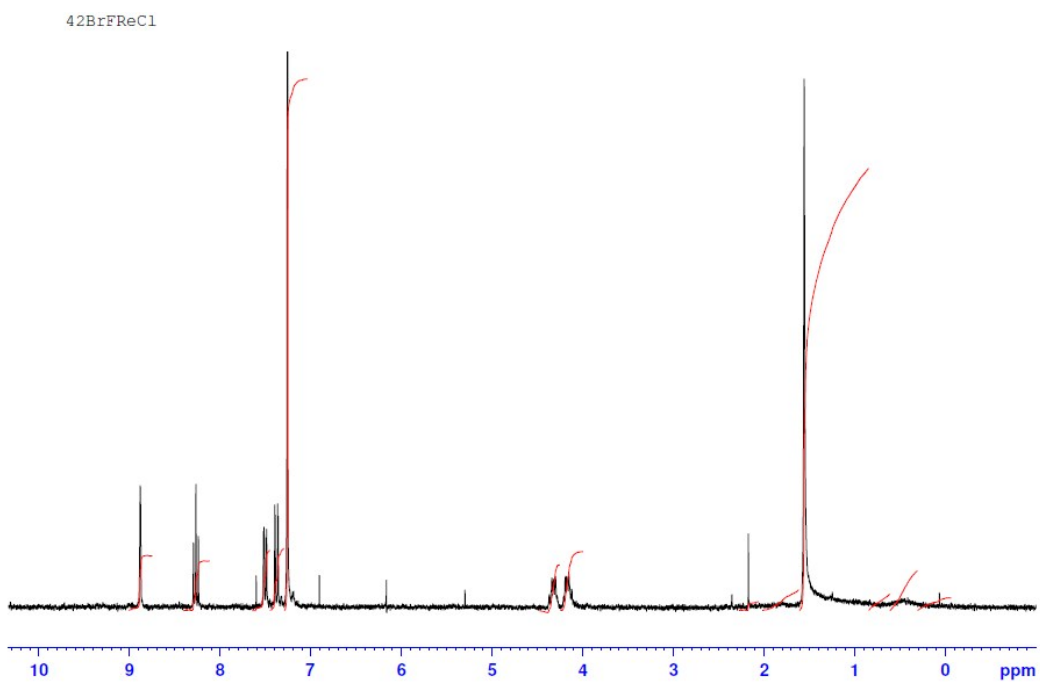


Fig. S6. $^1\text{H-NMR}$ spectrum of **C7** in CDCl_3 .

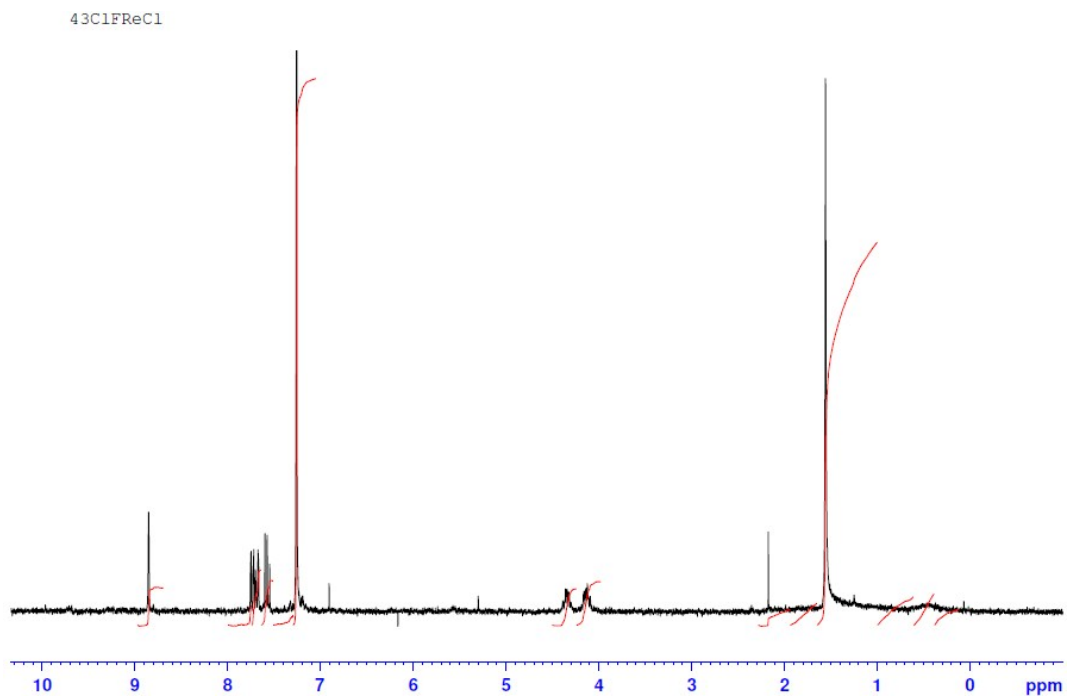


Fig. S7. ^1H -NMR spectrum of **C8** in CDCl_3 .

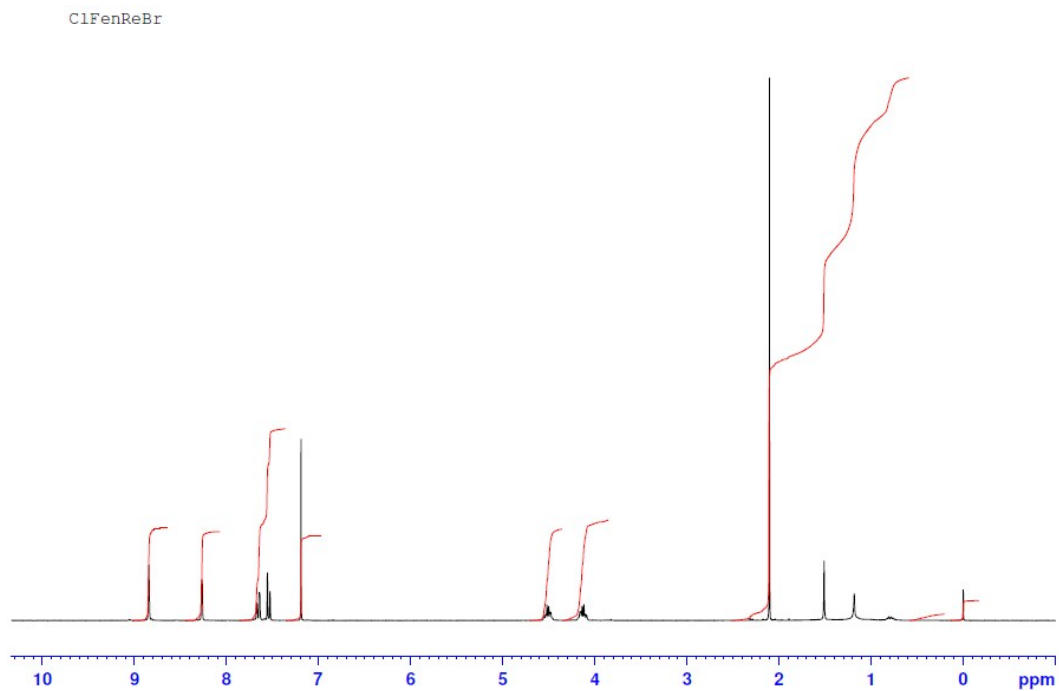


Fig. S8. ^1H -NMR spectrum of **C9** in CDCl_3 .

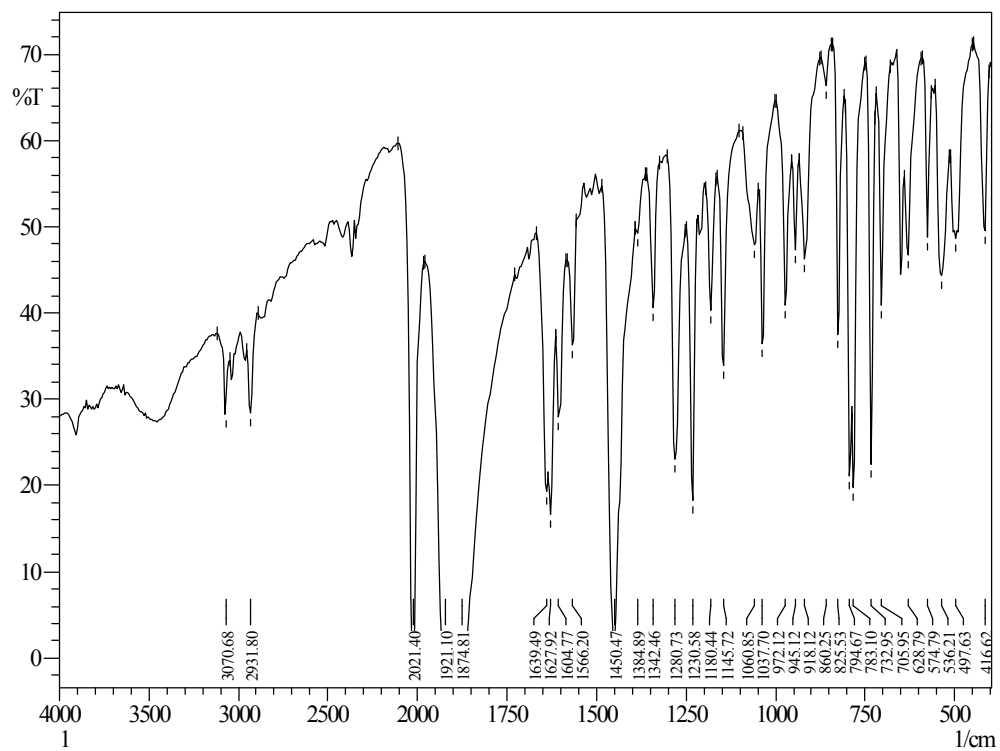


Fig. S9. FT-IR spectrum of 32ClFenReCl (C2).

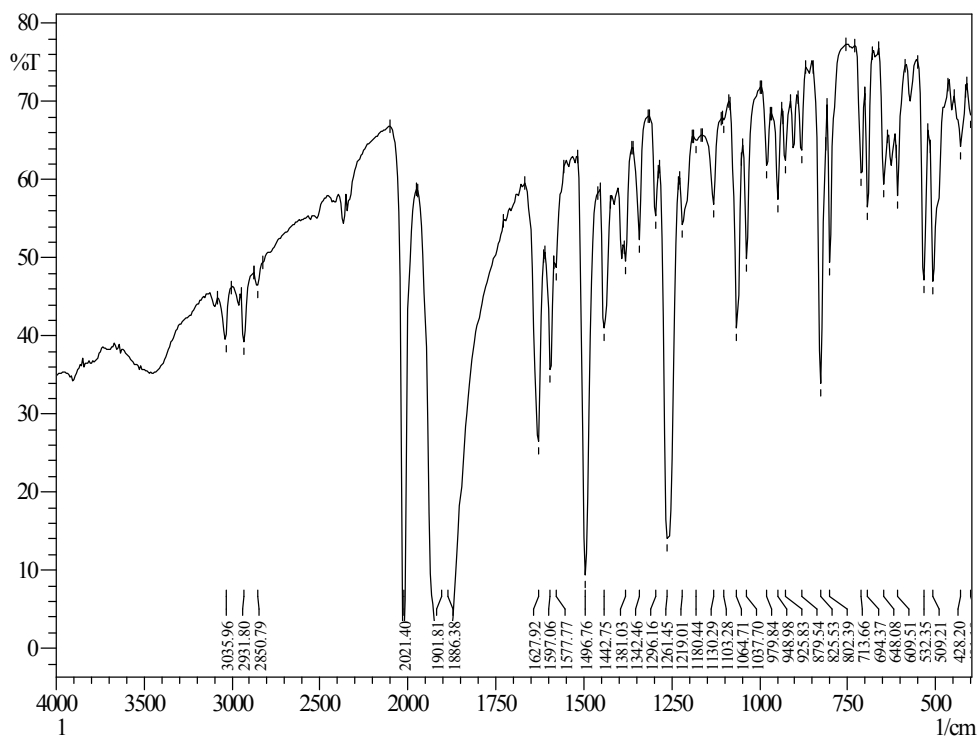


Fig. S10. FT-IR spectrum of 34ClFenReBr (C3).

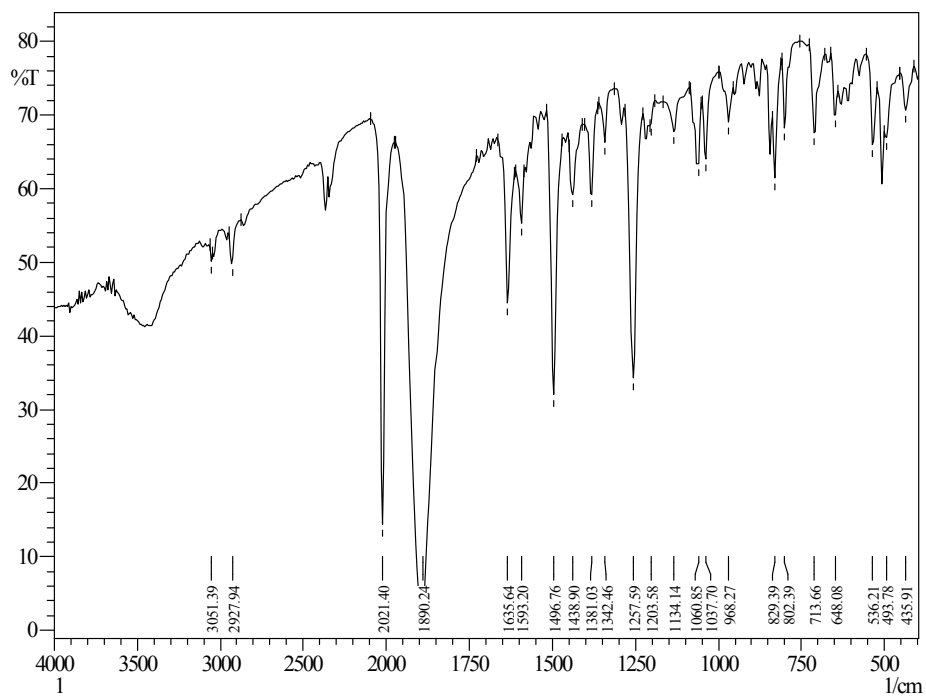


Fig. S11. FT-IR spectrum of 34ClFenReCl (C4).

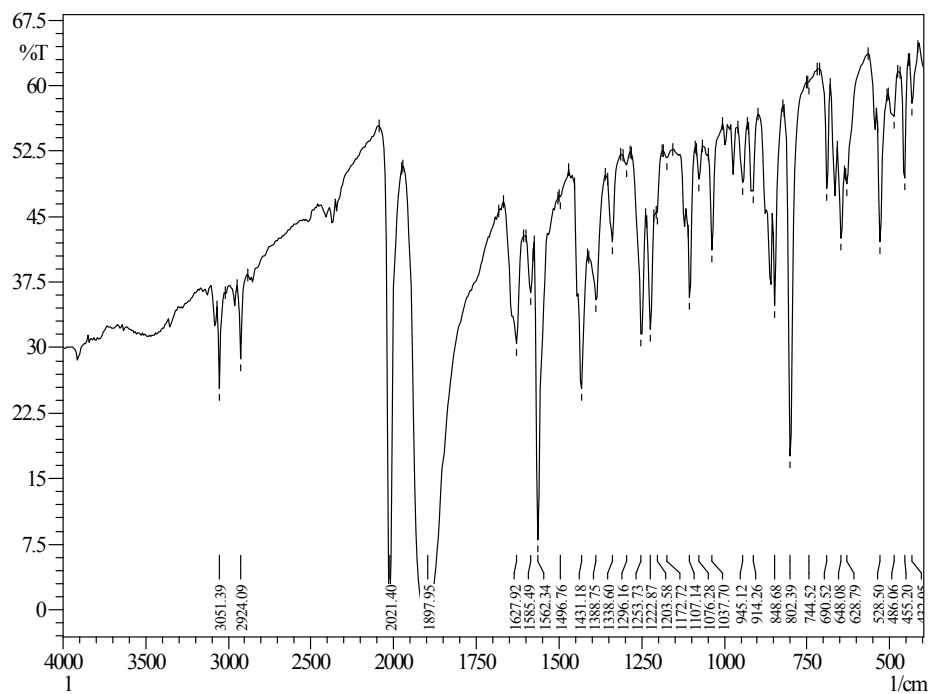


Fig. S12. FT-IR spectrum of 35ClenReBr (C5).

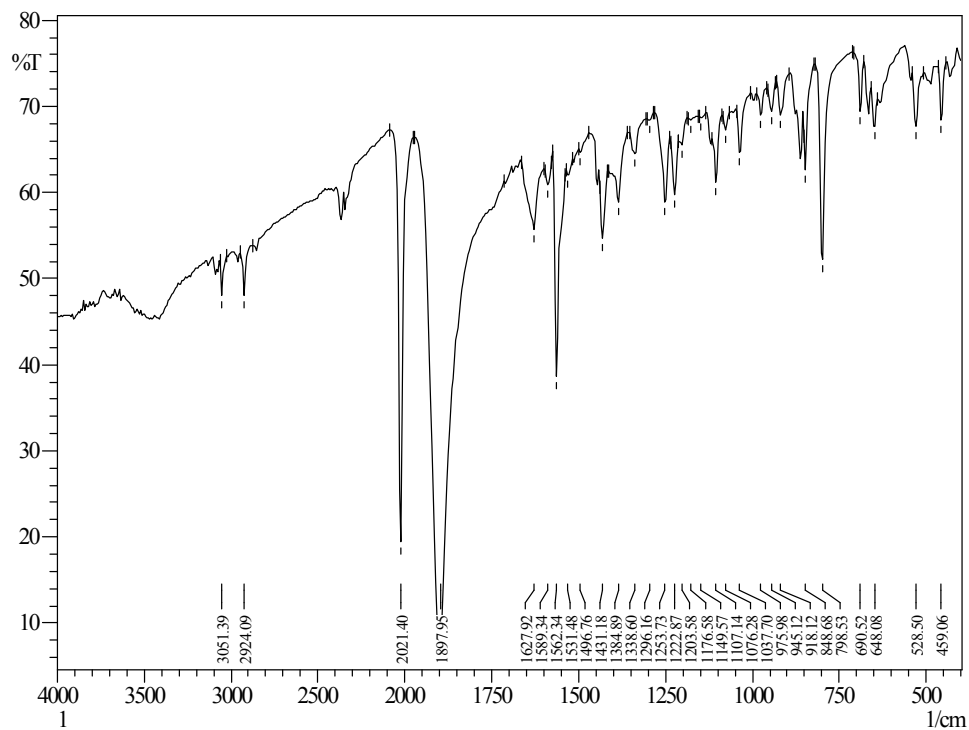


Fig. S13. FT-IR spectrum of 35ClenReCl (C6).

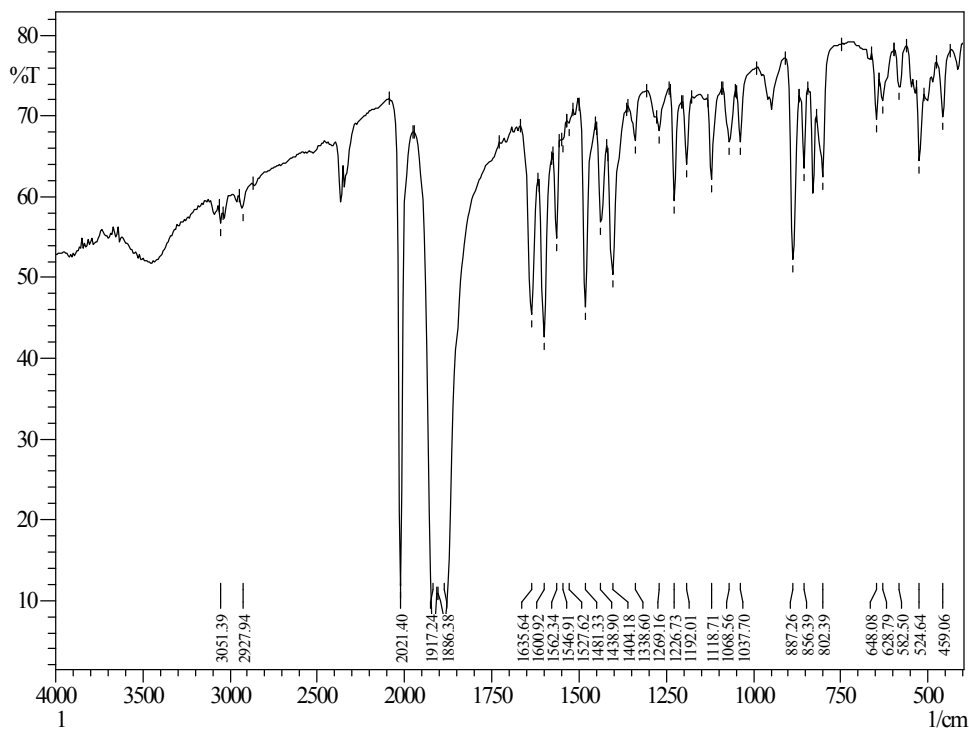


Fig. S14. FT-IR spectrum of 42BrFReCl (C7).

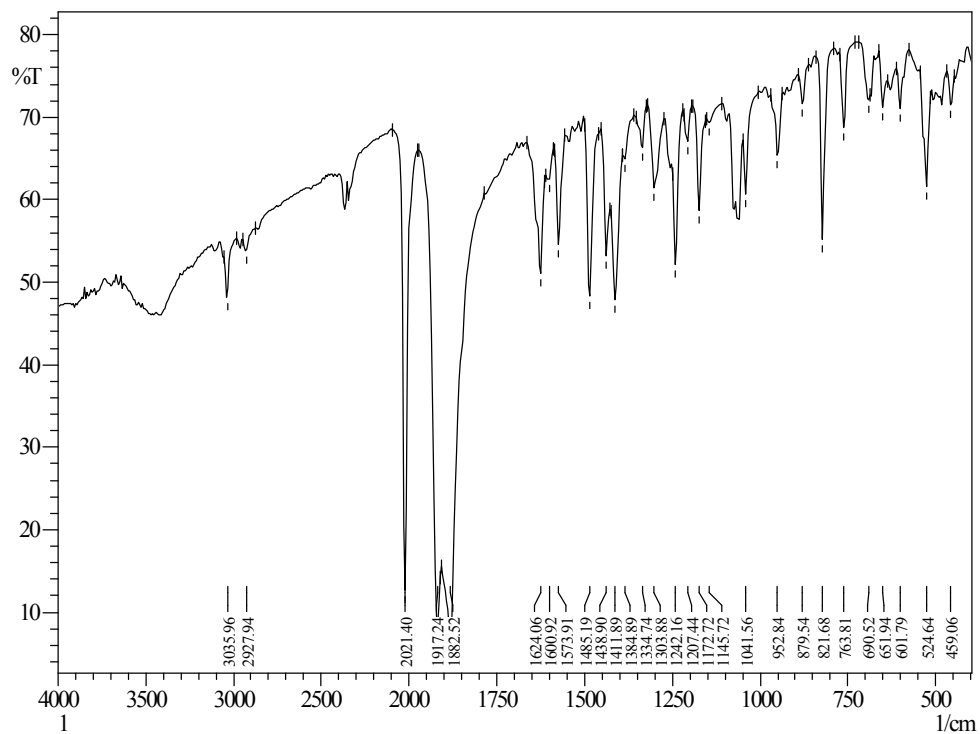


Fig. S15. FT-IR spectrum of **43ClFReCl (C8)**.

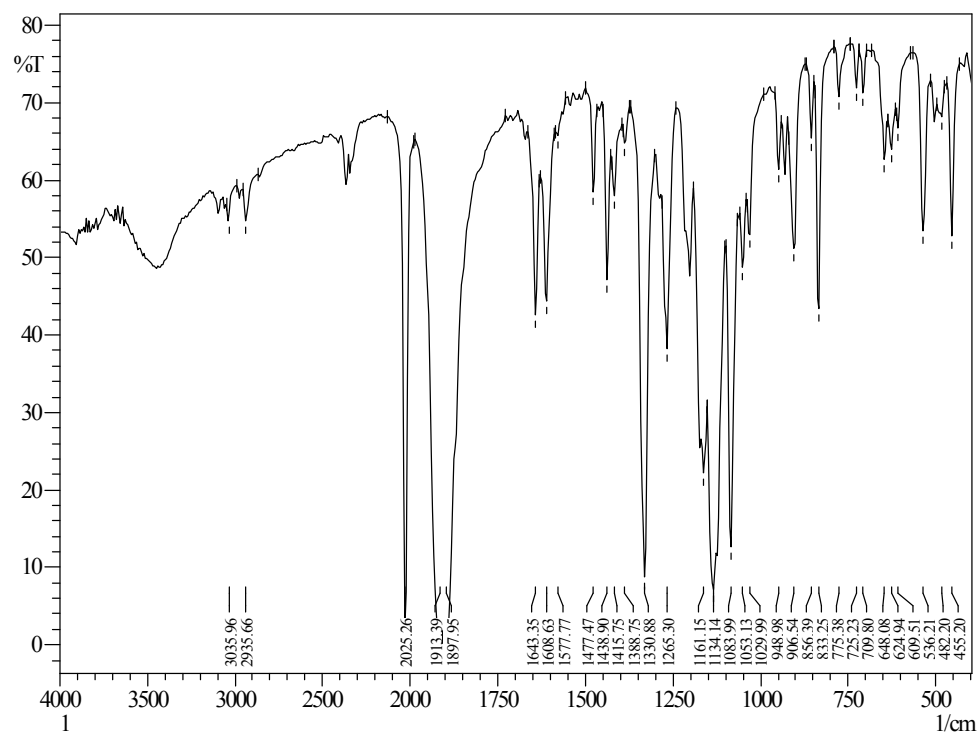


Fig. S16. FT-IR spectrum of **ClFenReBr (C9)**.

Table S1. Crystal data and structure refinement for C2 = 32ClFReCl

Identification code	C2	
Empirical formula	C19 H12 Cl3 F2 N2 O3 Re	
Formula weight	646.86	
Temperature	150(2) K	
Wavelength	0.71073 Å	
Crystal system	Triclinic	
Space group	<i>P</i> -1	
Unit cell dimensions	$a = 7.1480(2)$ Å	$\alpha = 105.7160(9)^\circ$
	$b = 9.2830(2)$ Å	$\beta = 98.7670(10)^\circ$
	$c = 17.0670(6)$ Å	$\gamma = 95.9490(14)^\circ$
Volume	1064.83(5) Å ³	
Z	2	
Density (calculated)	2.017 Mg/m ³	
Absorption coefficient	6.123 mm ⁻¹	
F(000)	616	
Crystal size	0.060 x 0.050 x 0.010 mm ³	
Theta range for data collection	2.917 to 27.502°	
Index ranges	-9 ≤ h ≤ 9, -12 ≤ k ≤ 12, -22 ≤ l ≤ 22	
Reflections collected	15268	
Independent reflections	4817 [R(int) = 0.0728]	
Completeness to theta = 25.242°	99.4 %	
Refinement method	Full-matrix least-squares on F ²	
Data / restraints / parameters	4817 / 0 / 271	
Goodness-of-fit on F ²	1.064	
Final R indices [I > 2σ(I)]	R1 = 0.0382, wR2 = 0.0913	
R indices (all data)	R1 = 0.0456, wR2 = 0.0957	
Largest diff. peak and hole	1.992 and -3.339 e.Å ⁻³	

Table S2. Crystal data and structure refinement for C3 = 34clfrebr

Identification code	C3	
Empirical formula	C19 H12 Br Cl2 F2 N2 O3 Re	
Formula weight	691.32	
Temperature	150(2) K	
Wavelength	0.71073 Å	
Crystal system	Triclinic	
Space group	<i>P</i> -1	
Unit cell dimensions	$a = 7.36000(10) \text{ \AA}$	$\alpha = 101.5080(10)^\circ$
	$b = 9.2080(3) \text{ \AA}$	$\beta = 94.970(2)^\circ$
	$c = 16.5900(5) \text{ \AA}$	$\gamma = 98.653(2)^\circ$
Volume	1081.25(5) Å ³	
Z	2	
Density (calculated)	2.123 Mg/m ³	
Absorption coefficient	7.754 mm ⁻¹	
F(000)	652	
Crystal size	0.200 x 0.050 x 0.050 mm ³	
Theta range for data collection	2.948 to 27.483°	
Index ranges	-9 ≤ h ≤ 9, -11 ≤ k ≤ 11, -21 ≤ l ≤ 21	
Reflections collected	15821	
Independent reflections	4940 [R(int) = 0.0512]	
Completeness to theta = 25.242°	99.8 %	
Refinement method	Full-matrix least-squares on F ²	
Data / restraints / parameters	4940 / 0 / 271	
Goodness-of-fit on F ²	1.279	
Final R indices [I > 2σ(I)]	R1 = 0.0272, wR2 = 0.0783	
R indices (all data)	R1 = 0.0339, wR2 = 0.0988	
Largest diff. peak and hole	1.511 and -2.575 e.Å ⁻³	

Table S3. Crystal data and structure refinement for C4 = 34clfrecl.

Identification code	C4	
Empirical formula	C19 H12 Cl3 F2 N2 O3 Re	
Formula weight	646.86	
Temperature	150(2) K	
Wavelength	0.71073 Å	
Crystal system	Monoclinic	
Space group	<i>P</i> 2 ₁ / <i>c</i>	
Unit cell dimensions	<i>a</i> = 15.4530(5) Å	$\alpha = 90^\circ$
	<i>b</i> = 7.0730(2) Å	$\beta = 126.1351(11)^\circ$
	<i>c</i> = 23.5290(8) Å	$\gamma = 90^\circ$
Volume	2076.98(12) Å ³	
Z	4	
Density (calculated)	2.069 Mg/m ³	
Absorption coefficient	6.278 mm ⁻¹	
F(000)	1232	
Crystal size	0.090 x 0.040 x 0.010 mm ³	
Theta range for data collection	3.073 to 27.519°	
Index ranges	-20 ≤ <i>h</i> ≤ 17, -9 ≤ <i>k</i> ≤ 8, -30 ≤ <i>l</i> ≤ 26	
Reflections collected	9932	
Independent reflections	4688 [R(int) = 0.0633]	
Completeness to theta = 25.242°	99.4 %	
Refinement method	Full-matrix least-squares on F ²	
Data / restraints / parameters	4688 / 0 / 271	
Goodness-of-fit on F ²	1.030	
Final R indices [I > 2σ(I)]	R1 = 0.0435, wR2 = 0.0957	
R indices (all data)	R1 = 0.0671, wR2 = 0.1081	
Largest diff. peak and hole	1.990 and -3.422 e.Å ⁻³	

Table S4. Crystal data and structure refinement for C5 = 35clenbr

Identification code	C5	
Empirical formula	C19 H12 Br Cl4 N2 O3 Re	
Formula weight	724.22	
Temperature	150(2) K	
Wavelength	0.71073 Å	
Crystal system	Triclinic	
Space group	<i>P</i> -1	
Unit cell dimensions	$a = 7.1653(3) \text{ \AA}$	$\alpha = 86.971(4)^\circ$
	$b = 10.1441(5) \text{ \AA}$	$\beta = 82.270(4)^\circ$
	$c = 16.1968(10) \text{ \AA}$	$\gamma = 71.257(4)^\circ$
Volume	1104.65(10) Å ³	
Z	2	
Density (calculated)	2.177 Mg/m ³	
Absorption coefficient	7.817 mm ⁻¹	
F(000)	684	
Crystal size	0.080 x 0.040 x 0.020 mm ³	
Theta range for data collection	3.424 to 29.262°	
Index ranges	-8<=h<=9, -12<=k<=13, -21<=l<=22	
Reflections collected	9299	
Independent reflections	5040 [R(int) = 0.0394]	
Completeness to theta = 25.242°	99.7 %	
Refinement method	Full-matrix least-squares on F ²	
Data / restraints / parameters	5040 / 0 / 271	
Goodness-of-fit on F ²	1.031	
Final R indices [I>2sigma(I)]	R1 = 0.0353, wR2 = 0.0691	
R indices (all data)	R1 = 0.0410, wR2 = 0.0722	
Largest diff. peak and hole	1.334 and -1.758 e.Å ⁻³	

Table S5. Crystal data and structure refinement for C6 = 35clencl

Identification code	C6	
Empirical formula	C19 H12 Cl5 N2 O3 Re	
Formula weight	679.76	
Temperature	150(2) K	
Wavelength	0.71073 Å	
Crystal system	Monoclinic	
Space group	<i>P</i> 2 ₁ / <i>c</i>	
Unit cell dimensions	<i>a</i> = 7.12100(10) Å	$\alpha = 90^\circ$
	<i>b</i> = 33.7880(7) Å	$\beta = 96.0240(8)^\circ$
	<i>c</i> = 9.4780(2) Å	$\gamma = 90^\circ$
Volume	2267.86(7) Å ³	
Z	4	
Density (calculated)	1.991 Mg/m ³	
Absorption coefficient	5.971 mm ⁻¹	
F(000)	1296	
Crystal size	0.060 x 0.030 x 0.020 mm ³	
Theta range for data collection	2.939 to 27.475°	
Index ranges	-8 ≤ <i>h</i> ≤ 9, -43 ≤ <i>k</i> ≤ 27, -12 ≤ <i>l</i> ≤ 12	
Reflections collected	13899	
Independent reflections	5136 [R(int) = 0.0561]	
Completeness to theta = 25.242°	99.3 %	
Refinement method	Full-matrix least-squares on F ²	
Data / restraints / parameters	5136 / 0 / 271	
Goodness-of-fit on F ²	1.035	
Final R indices [I > 2σ(I)]	R1 = 0.0339, wR2 = 0.0559	
R indices (all data)	R1 = 0.0642, wR2 = 0.0655	
Largest diff. peak and hole	1.650 and -1.628 e.Å ⁻³	

Table S6. Crystal data and structure refinement for C7 = 42BrFReCl

Identification code	C7	
Empirical formula	C19 H12 Br2 Cl F2 N2 O3 Re	
Formula weight	735.78	
Temperature	150(2) K	
Wavelength	0.71073 Å	
Crystal system	Triclinic	
Space group	<i>P</i> -1	
Unit cell dimensions	$a = 7.3756(4)$ Å	$\alpha = 98.004(4)^\circ$
	$b = 8.8914(4)$ Å	$\beta = 90.442(5)^\circ$
	$c = 16.9636(10)$ Å	$\gamma = 105.113(4)^\circ$
Volume	1062.40(10) Å ³	
Z	2	
Density (calculated)	2.300 Mg/m ³	
Absorption coefficient	9.647 mm ⁻¹	
F(000)	688	
Crystal size	0.100 x 0.060 x 0.020 mm ³	
Theta range for data collection	3.357 to 27.500°	
Index ranges	-9 ≤ h ≤ 9, -11 ≤ k ≤ 11, -22 ≤ l ≤ 22	
Reflections collected	15534	
Independent reflections	4862 [R(int) = 0.0526]	
Completeness to theta = 25.242°	99.7 %	
Refinement method	Full-matrix least-squares on F ²	
Data / restraints / parameters	4862 / 0 / 281	
Goodness-of-fit on F ²	1.023	
Final R indices [I > 2σ(I)]	R1 = 0.0527, wR2 = 0.1244	
R indices (all data)	R1 = 0.0727, wR2 = 0.1355	
Largest diff. peak and hole	3.252 and -1.709 e.Å ⁻³	

Table S7. Crystal data and structure refinement for C8 = 43ClFReCl

Identification code	C8	
Empirical formula	C38 H24 Cl6 F4 N4 O6 Re2	
Formula weight	1293.71	
Temperature	150(2) K	
Wavelength	0.71073 Å	
Crystal system	Triclinic	
Space group	P-1	
Unit cell dimensions	$a = 7.3006(5) \text{ \AA}$	$a = 104.105(5)^\circ$
	$b = 11.5980(7) \text{ \AA}$	$b = 97.855(5)^\circ$
	$c = 12.6789(8) \text{ \AA}$	$g = 96.998(5)^\circ$
Volume	1017.88(12) Å ³	
Z	1	
Density (calculated)	2.111 Mg/m ³	
Absorption coefficient	6.405 mm ⁻¹	
F(000)	616	
Crystal size	0.100 x 0.060 x 0.030 mm ³	
Theta range for data collection	3.364 to 29.201°	
Index ranges	-9<=h<=10, -15<=k<=15, -17<=l<=17	
Reflections collected	8612	
Independent reflections	4683 [R(int) = 0.0395]	
Completeness to theta = 25.242°	99.8 %	
Refinement method	Full-matrix least-squares on F ²	
Data / restraints / parameters	4683 / 0 / 271	
Goodness-of-fit on F ²	1.019	
Final R indices [I>2sigma(I)]	R1 = 0.0321, wR2 = 0.0557	
R indices (all data)	R1 = 0.0361, wR2 = 0.0583	
Largest diff. peak and hole	1.350 and -1.345 e.Å ⁻³	

Table S8. Crystal data and structure refinement for C9 = ClFReBr

Identification code	C9	
Empirical formula	C ₂₁ H ₁₂ Br Cl ₂ F ₆ N ₂ O ₃ Re	
Formula weight	791.34	
Temperature	150(2) K	
Wavelength	0.71073 Å	
Crystal system	Monoclinic	
Space group	<i>P</i> 2 ₁ / <i>c</i>	
Unit cell dimensions	<i>a</i> = 7.2547(4) Å	$\alpha = 90^\circ$
	<i>b</i> = 26.9040(16) Å	$\beta = 93.127(6)^\circ$
	<i>c</i> = 12.6293(7) Å	$\gamma = 90^\circ$
Volume	2461.3(2) Å ³	
Z	4	
Density (calculated)	2.136 Mg/m ³	
Absorption coefficient	6.850 mm ⁻¹	
F(000)	1496	
Crystal size	0.120 x 0.080 x 0.050 mm ³	
Theta range for data collection	3.404 to 25.997°	
Index ranges	-8 ≤ <i>h</i> ≤ 8, -33 ≤ <i>k</i> ≤ 33, -15 ≤ <i>l</i> ≤ 15	
Reflections collected	21636	
Independent reflections	4820 [R(int) = 0.0477]	
Completeness to theta = 25.242°	99.8 %	
Refinement method	Full-matrix least-squares on F ²	
Data / restraints / parameters	4820 / 0 / 325	
Goodness-of-fit on F ²	1.098	
Final R indices [I > 2σ(I)]	R1 = 0.0331, wR2 = 0.0542	
R indices (all data)	R1 = 0.0442, wR2 = 0.0571	
Largest diff. peak and hole	0.880 and -0.858 e.Å ⁻³	

Table S9. Crystal data and structure refinement for C10 = ClFReBr'.

Identification code	C10	
Empirical formula	C ₂₁ H ₁₂ Br Cl ₂ F ₆ N ₂ O ₃ Re	
Formula weight	791.34	
Temperature	100(2) K	
Wavelength	0.71073 Å	
Crystal system	Monoclinic	
Space group	<i>P</i> 2 ₁ / <i>c</i>	
Unit cell dimensions	a = 9.6938(1)	$\alpha = 90^\circ$
	b = 12.9012(2)	$\beta = 91.1190(10)^\circ$
	c = 22.2519(3)	$\gamma = 90^\circ$
Volume	2782.33(6) Å ³	
Z	4	
Density (calculated)	1.889 Mg/m ³	
Absorption coefficient	6.060 mm ⁻¹	
F(000)	1496	
Crystal size	0.314 x 0.226 x 0.050 mm ³	
Theta range for data collection	1.825 to 30.856°	
Index ranges	-13 ≤ h ≤ 13, -18 ≤ k ≤ 18, -32 ≤ l ≤ 29	
Reflections collected	36476	
Independent reflections	8709 [R(int) = 0.0518]	
Completeness to theta = 25.242°	99.9 %	
Refinement method	Full-matrix least-squares on F ²	
Data / restraints / parameters	8709 / 0 / 325	
Goodness-of-fit on F ²	1.061	
Final R indices [I > 2σ(I)]	R1 = 0.0381, wR2 = 0.0905	
R indices (all data)	R1 = 0.0627, wR2 = 0.1031	
Largest diff. peak and hole	1.169 and -1.882 e.Å ⁻³	

Calculated electrostatic potential surfaces for complexes C1-C10 with G09-BP86-D3/def2-TZVP. Colour scale: positive (blue = +0.045 a.u.); negative (red = -0.045 a.u.).

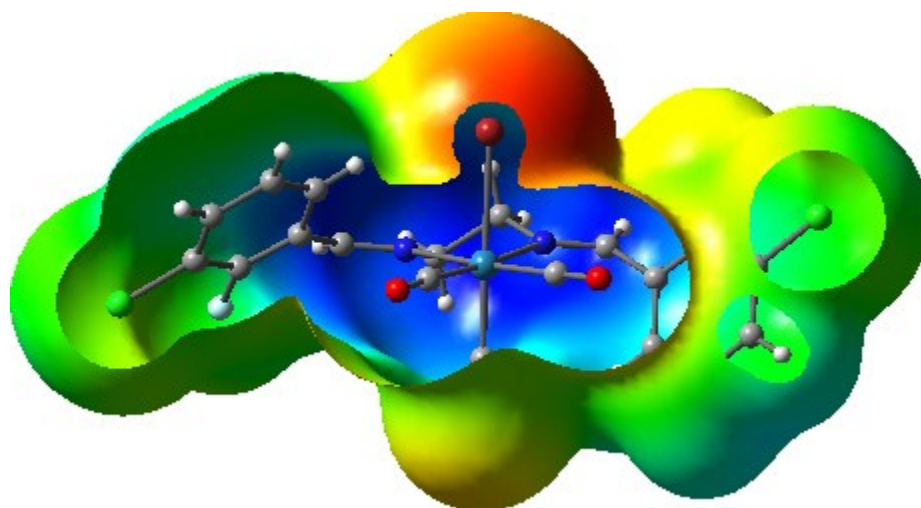


Fig. S17. MEP of C1 [isovalue at -0.045 to 0.045].

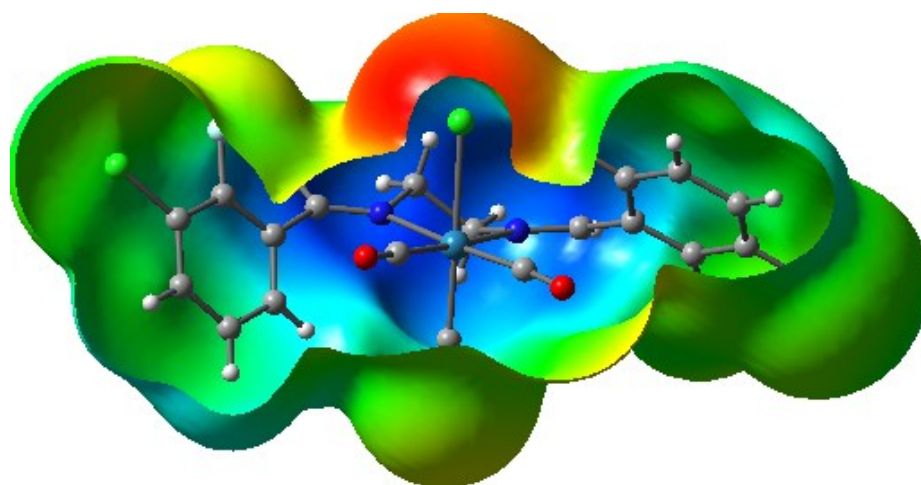


Fig. S18. MEP of C2 [isovalue at -0.045 to 0.045].

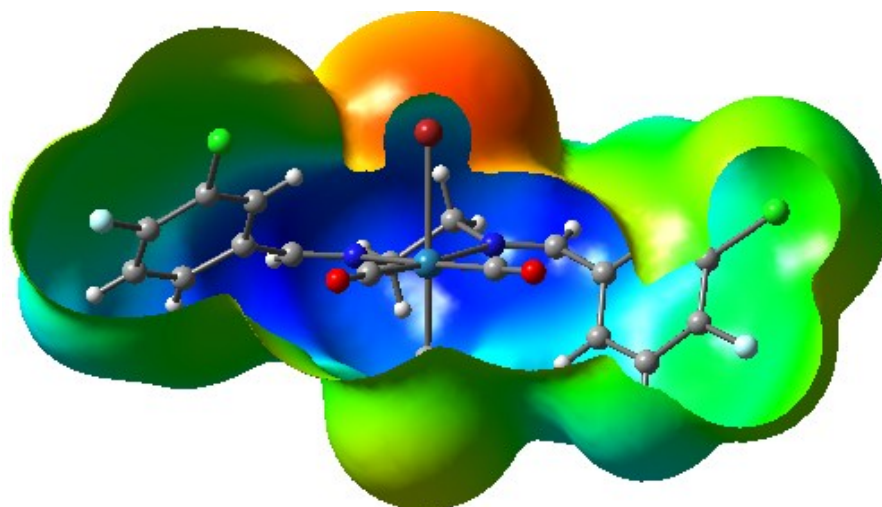


Fig. S19. MEP of C3 [isovalue at -0.045 to 0.045].

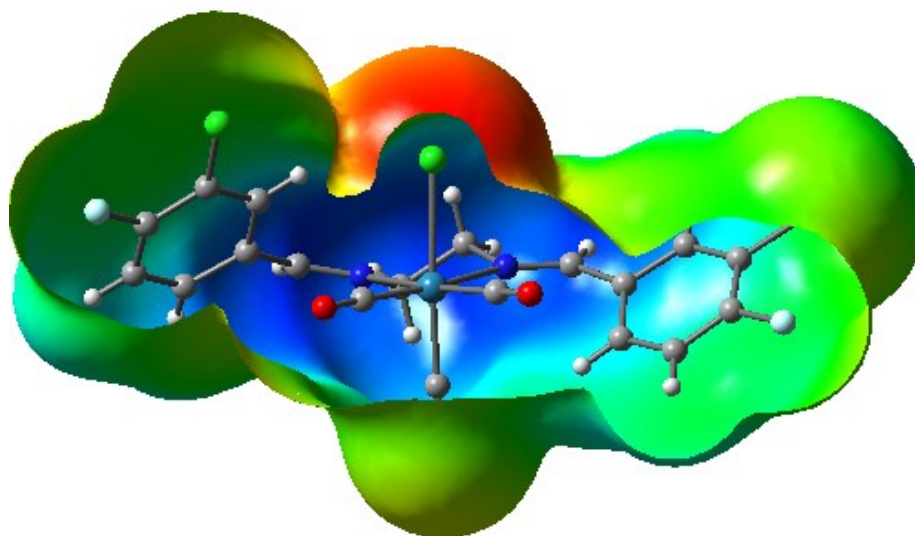


Fig. S20. MEP of C4 [isovalue at -0.045 to 0.045].

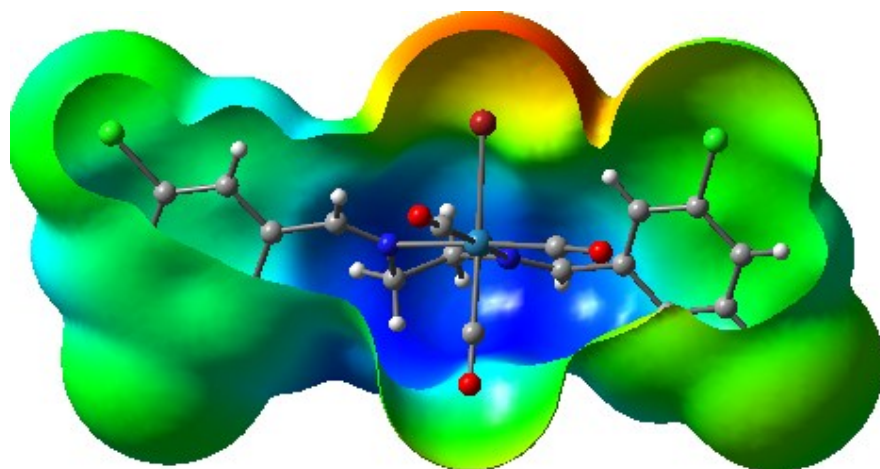


Fig. S21. MEP of C5 [isovalue at -0.045 to 0.045].

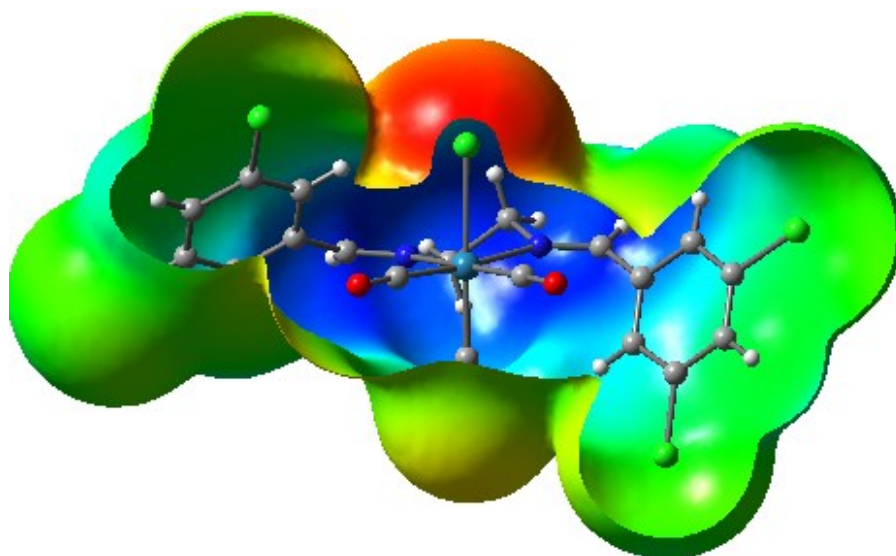


Fig. S22. MEP of C6 [isovalue at -0.045 to 0.045].

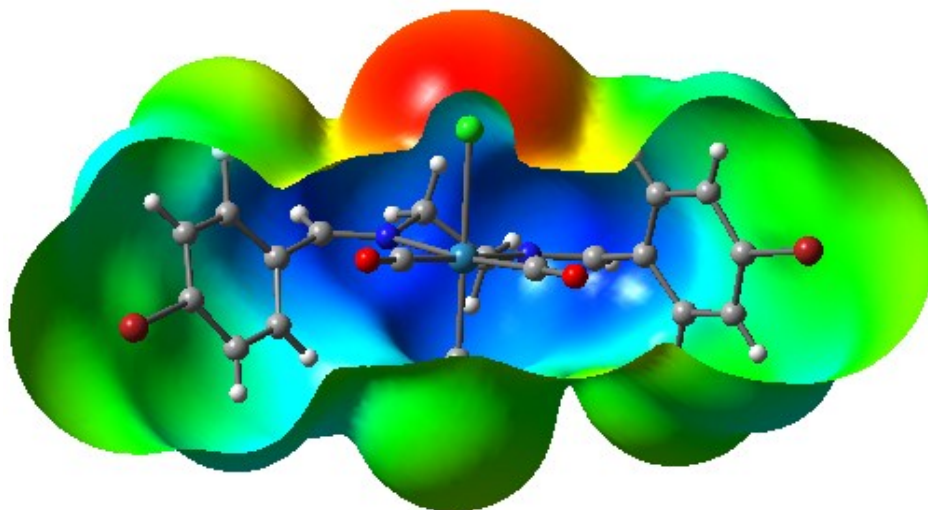


Fig. S23. MEP of C7 [isovalue at -0.045 to 0.045].

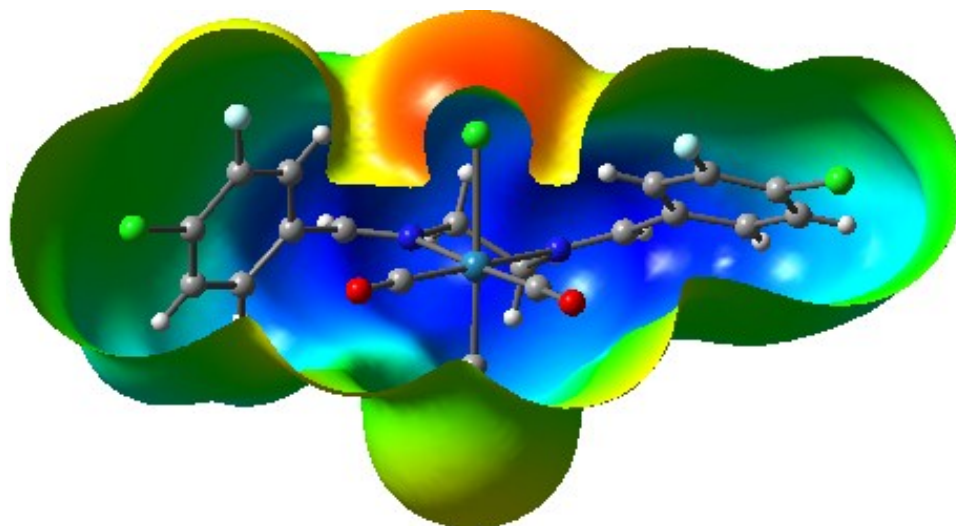


Fig. S24. MEP of C8 [isovalue at -0.045 to 0.045].

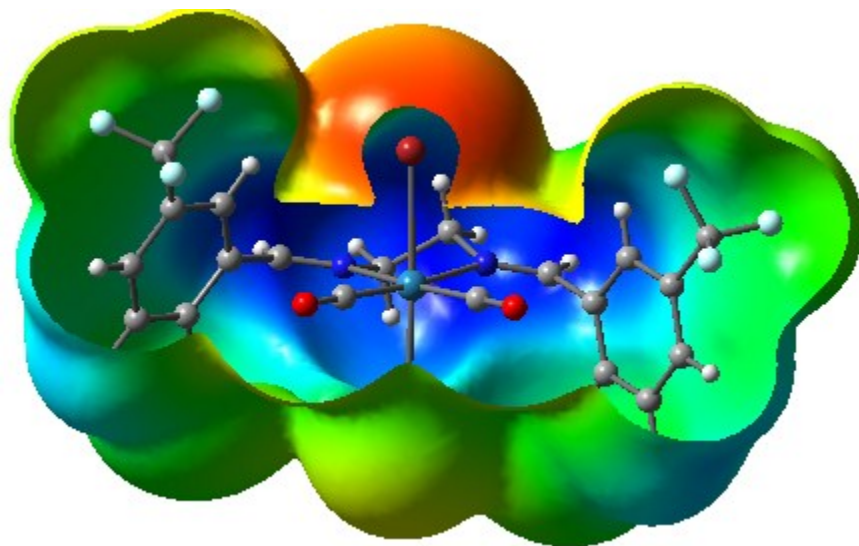


Fig. S25. MEP of C9 [isovalue at -0.045 to 0.045].

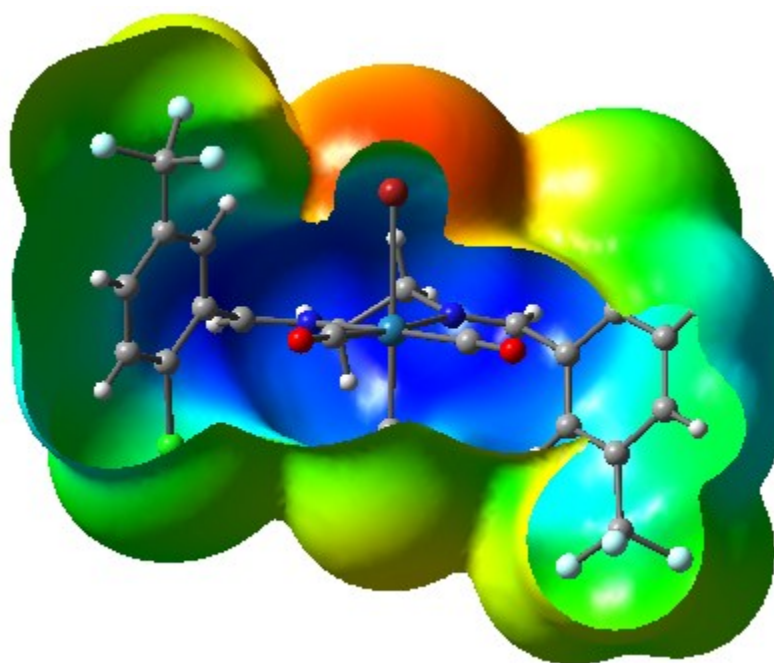


Fig. S26. MEP of C10 [isovalue at -0.045 to 0.045].

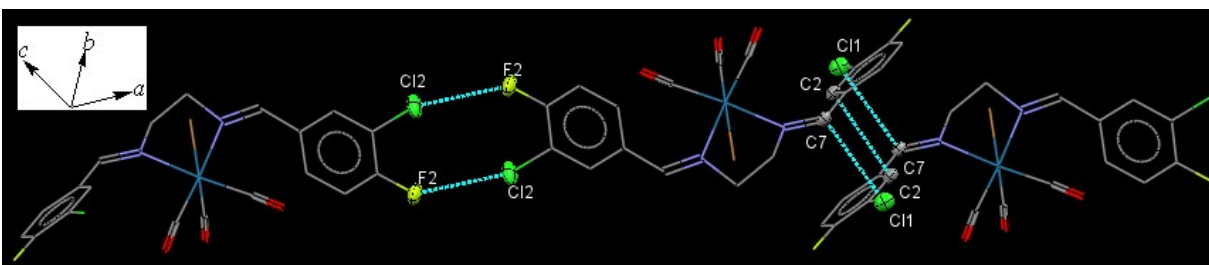


Fig. S27. Individual dimer formation in **C3** through the pair of intermolecular Cl...F interactions supported by C...Cl and C...C contacts.

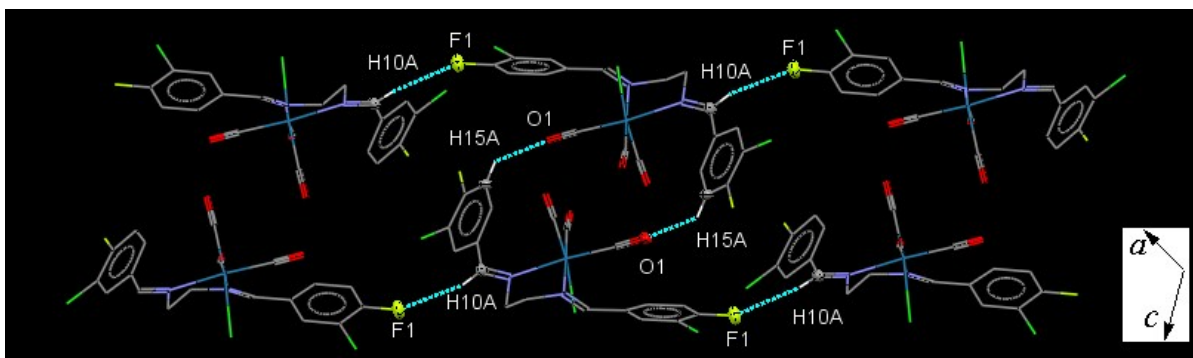


Fig. S28. Part of the crystal packing of **C4** viewed down the *b*-axis, showing head-to-tail individual dimer formation through C-H...O, further supported by the intermolecular C-H...F interactions.

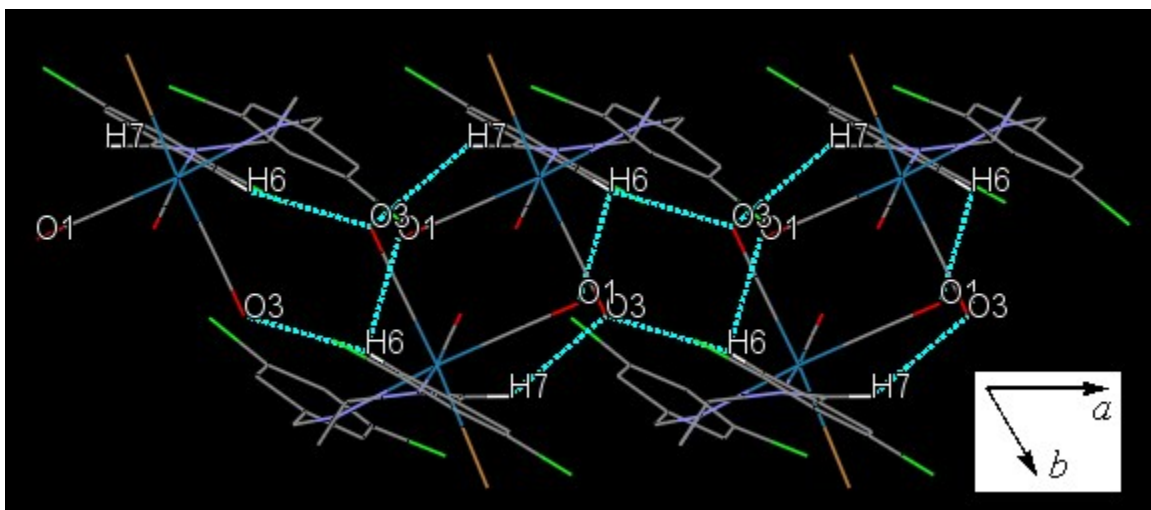


Fig. S29. Pair of intermolecular C7-H7...O3 and C6-H6...O1 hydrogen bonds form a centrosymmetric dimer in **C5**, linking molecules into an infinite chain along the *a*-axis.

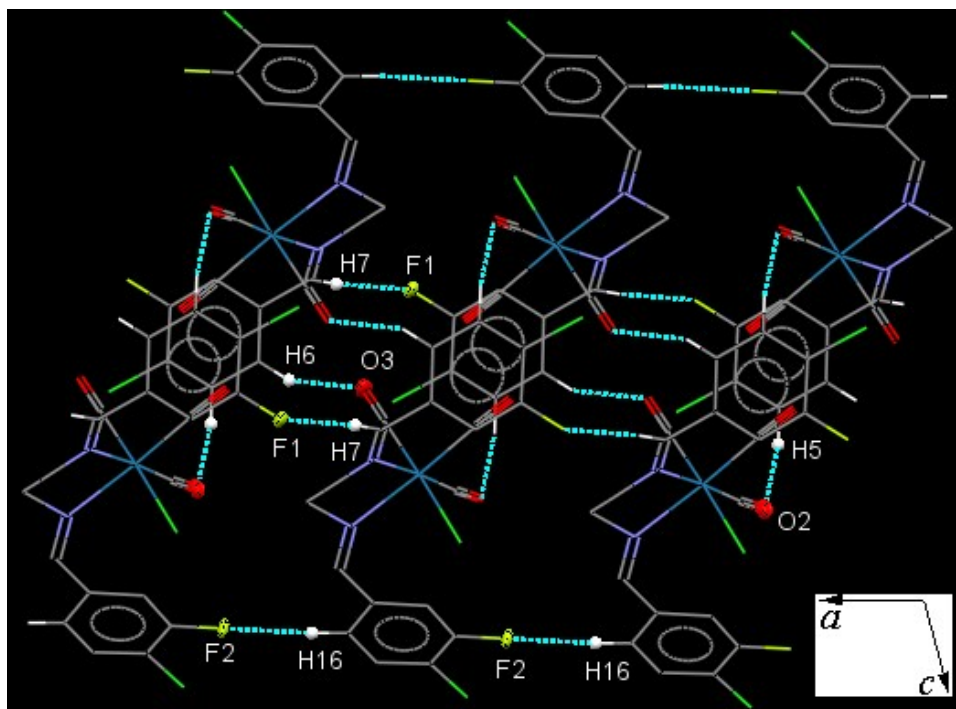


Fig. S30. Part of the crystal packing of **C8**, showing interconnected chains of neighboring molecules through the intermolecular $C1 \cdots Br$ halogen bond along $[110]$ direction.

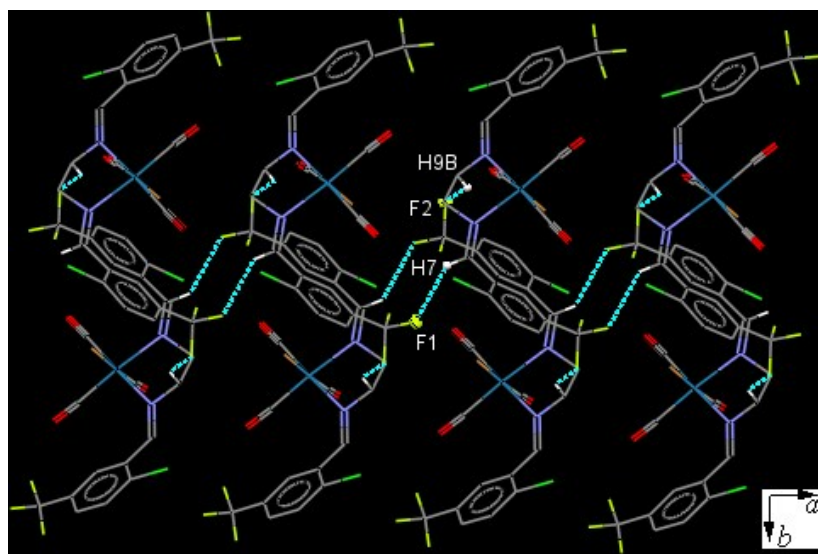


Fig. S31. Part of the packing of **C9**, showing connection of neighboring molecules into one-dimensional extended chain along the c -axis through $C-H \cdots F$ interactions.

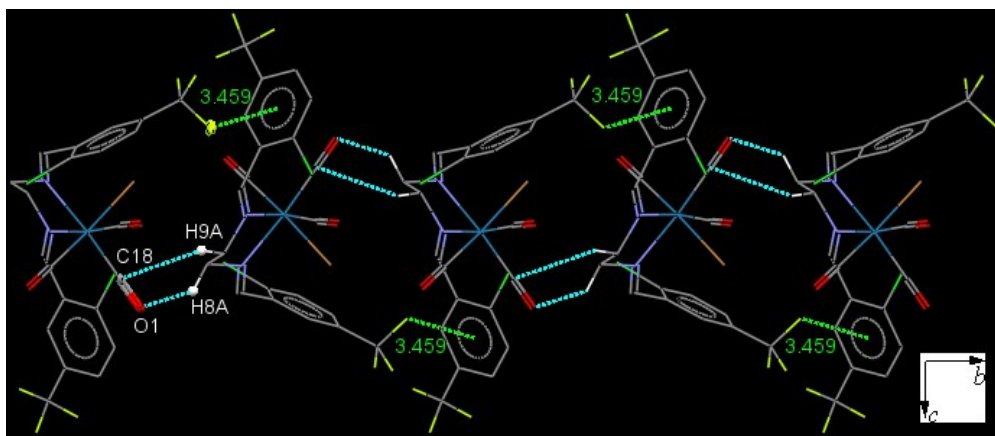


Fig. S32. One-dimensional extended chain of **C10** along the *b*-axis through intermolecular C–F \cdots π , C–H \cdots O and C–H \cdots π interactions.

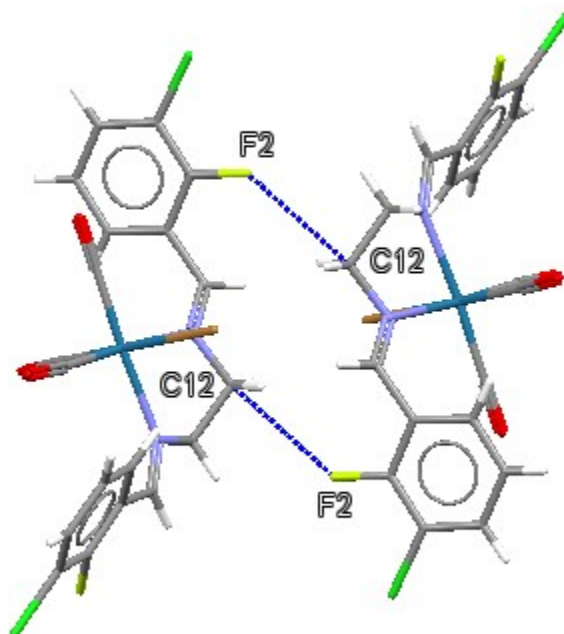


Fig. S33a. Dimer of **C1** formed from crystallographic coordinates.

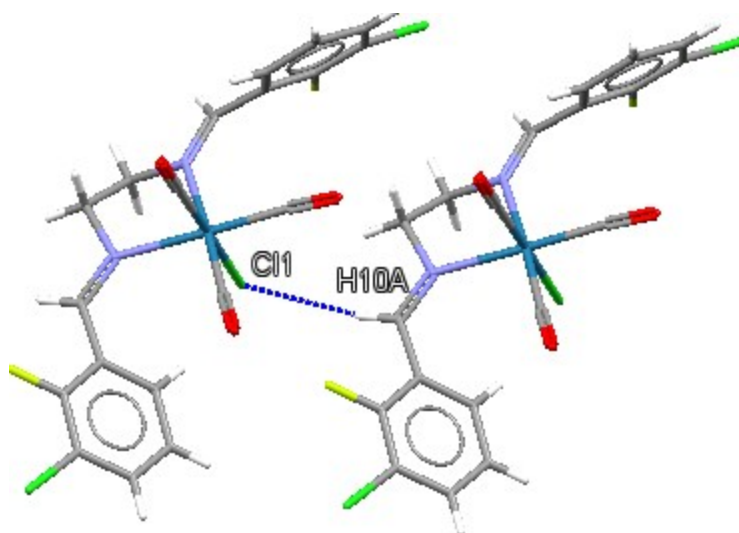


Fig. S33b. Dimer of C2 formed from crystallographic coordinates.

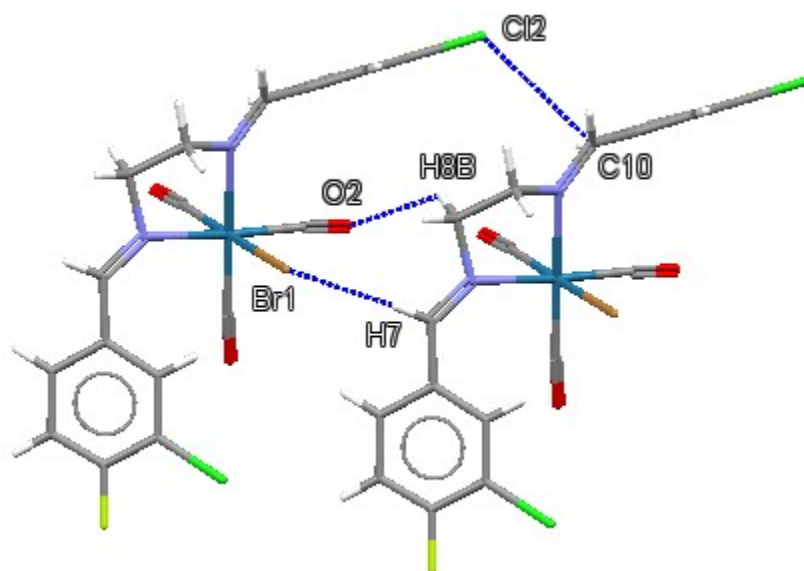


Fig. S33c. Dimer of C3 formed from crystallographic coordinates.

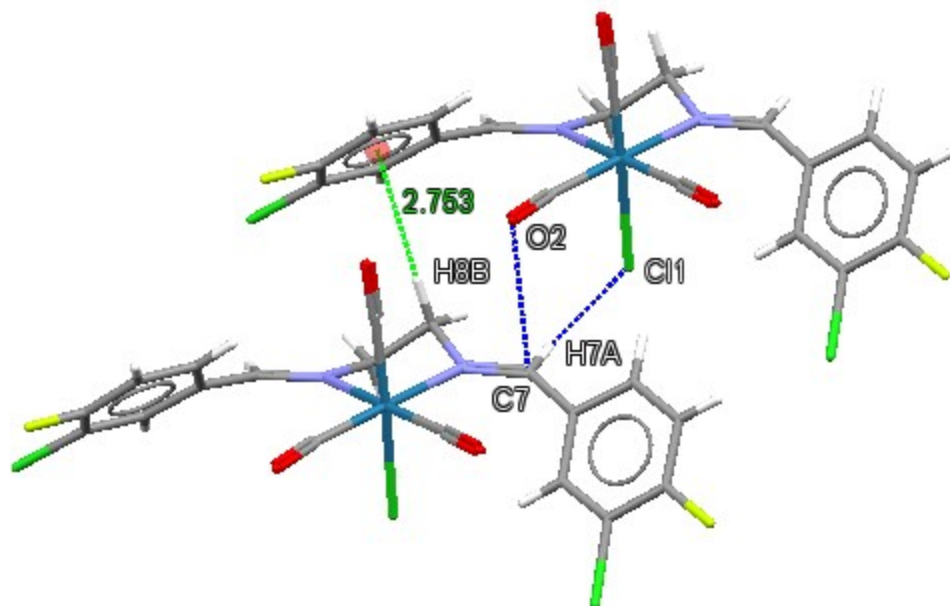


Fig. S33d. Dimer of C4 formed from crystallographic coordinates.

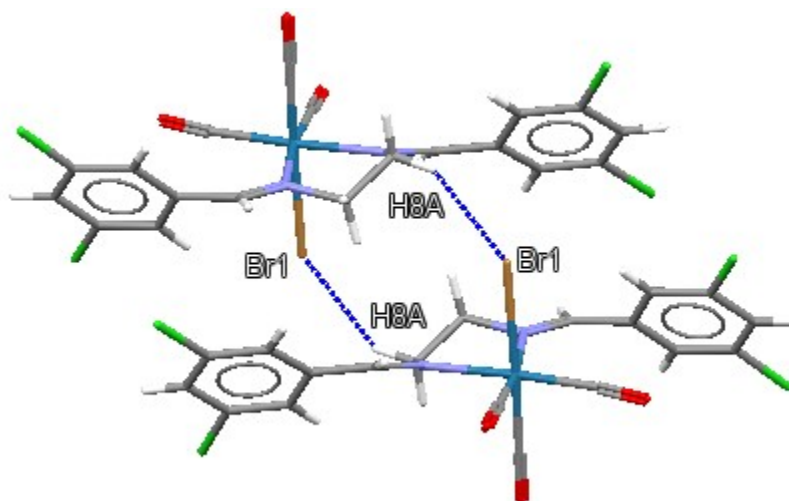


Fig. S33e. Dimer of C5 formed from crystallographic coordinates.

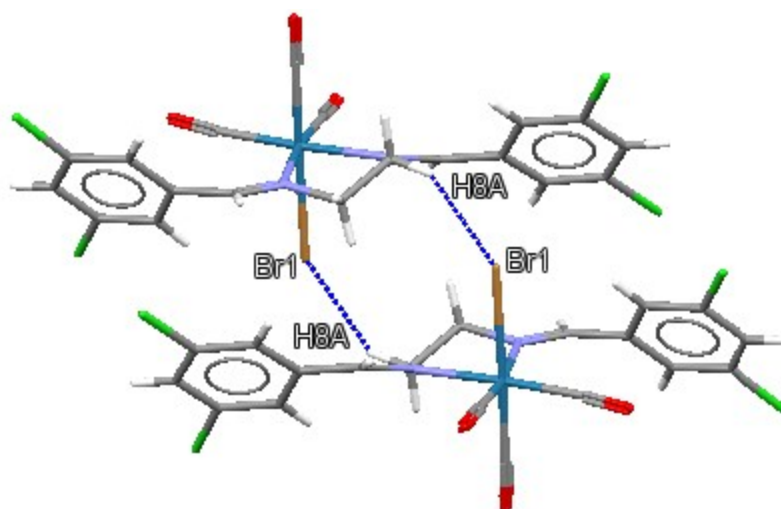


Fig. S33f. Dimer of C5 formed from crystallographic coordinates.

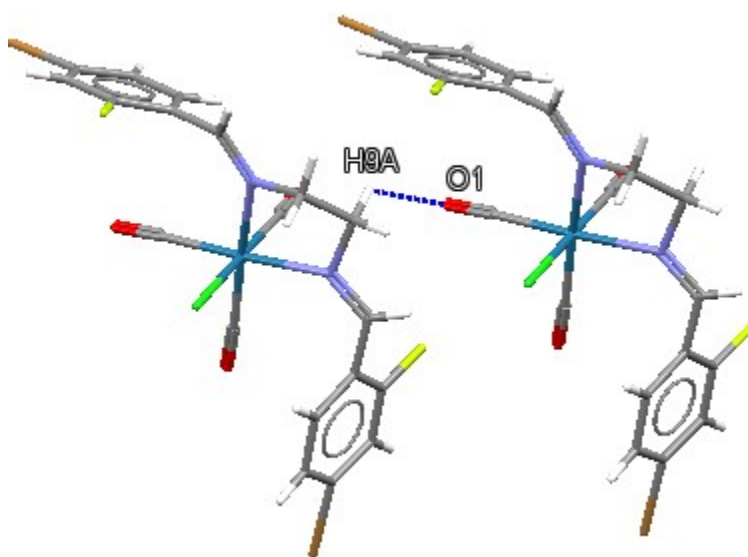


Fig. S33g. Dimer of C7 formed from crystallographic coordinates.

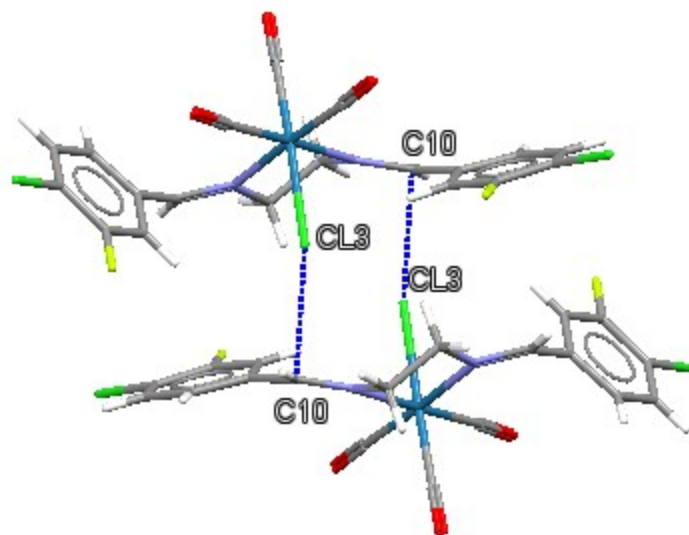


Fig. S33h. Dimer of C8 formed from crystallographic coordinates.

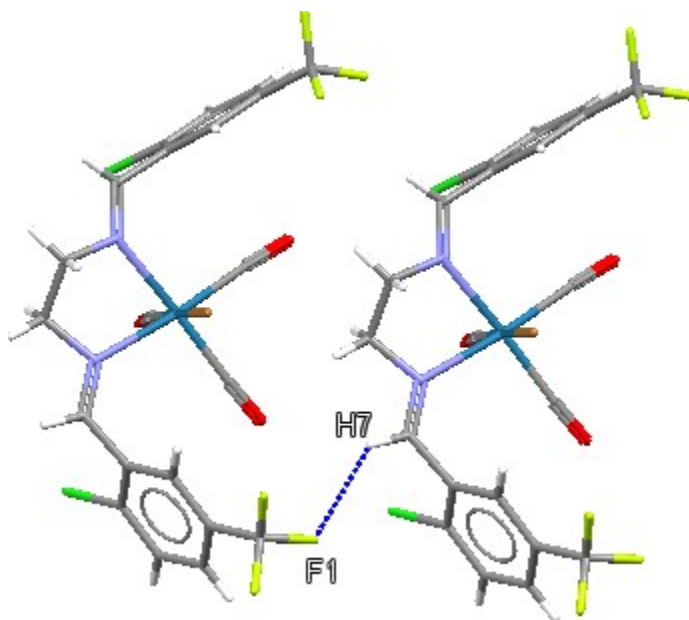


Fig. S33i. Dimer of C9 formed from crystallographic coordinates.

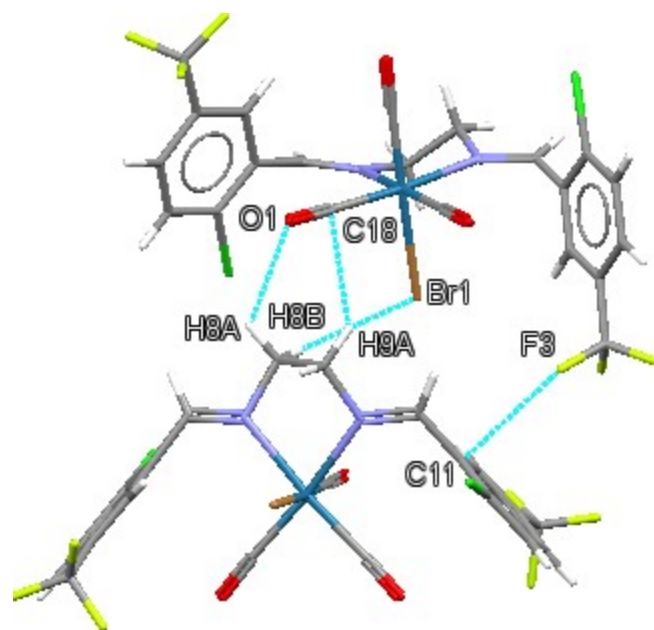


Fig. S33j. Dimer of C10 formed from crystallographic coordinates.

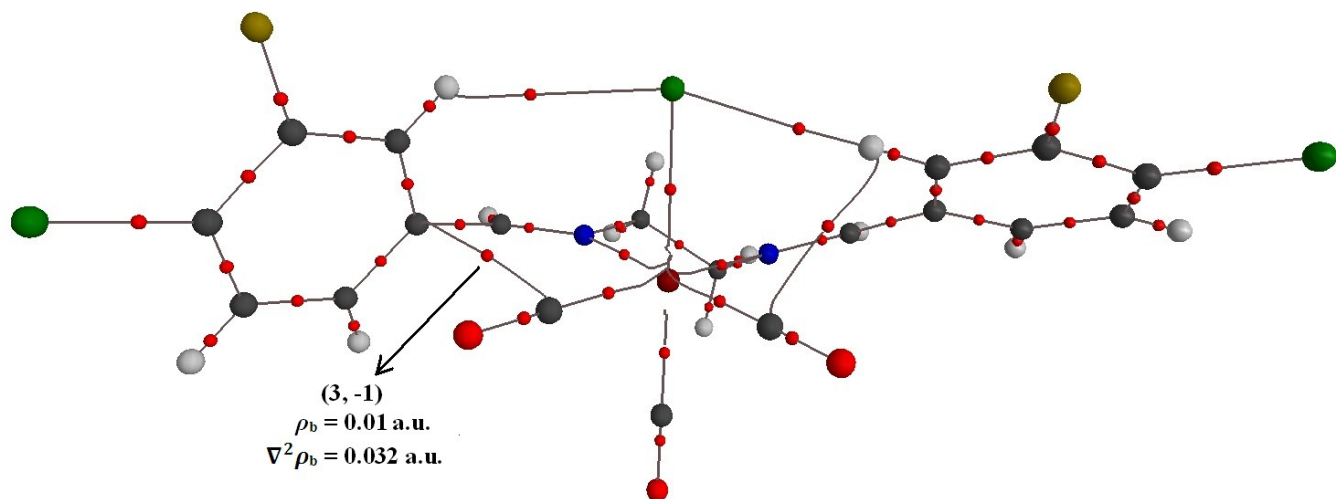


Fig. S34a. The bond critical points (BCPs) with their bond paths in **C8**. The specified BCP shows the interaction of the carbonyl group with the arene ring.

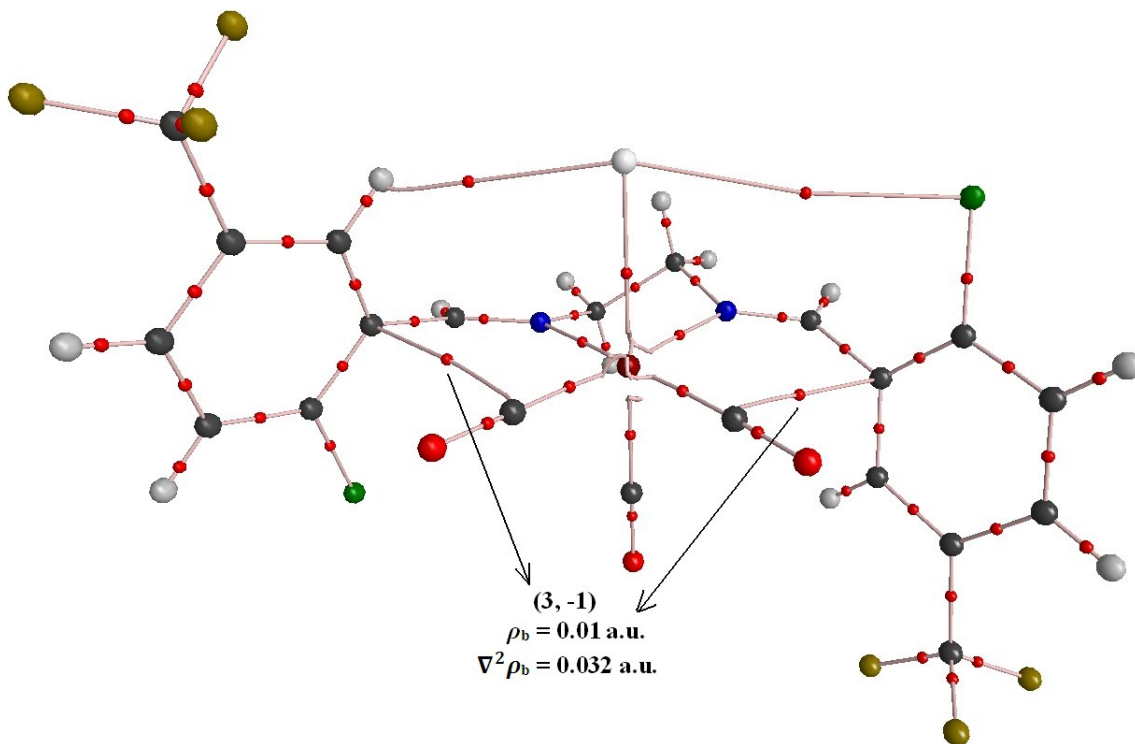


Fig. S34b. The bond critical points (BCPs) with their bond paths in **C10**. The specified BCP shows the interaction of the carbonyl group with the arene ring.

Fig. S35a-o:

The intermolecular interaction iso-surfaces generated by NCIPLOT for $s = 0.3$ and $-0.03 < \rho \cdot \text{sign}(\lambda_2) < +0.03$ [colour scale: attractive (blue) \rightarrow repulsive (red)] (top) and plots of $\rho \cdot \text{sign}(\lambda_2)$ vs. reduced density gradient highlighting the favorable interaction corresponding to the halogen bond (down).

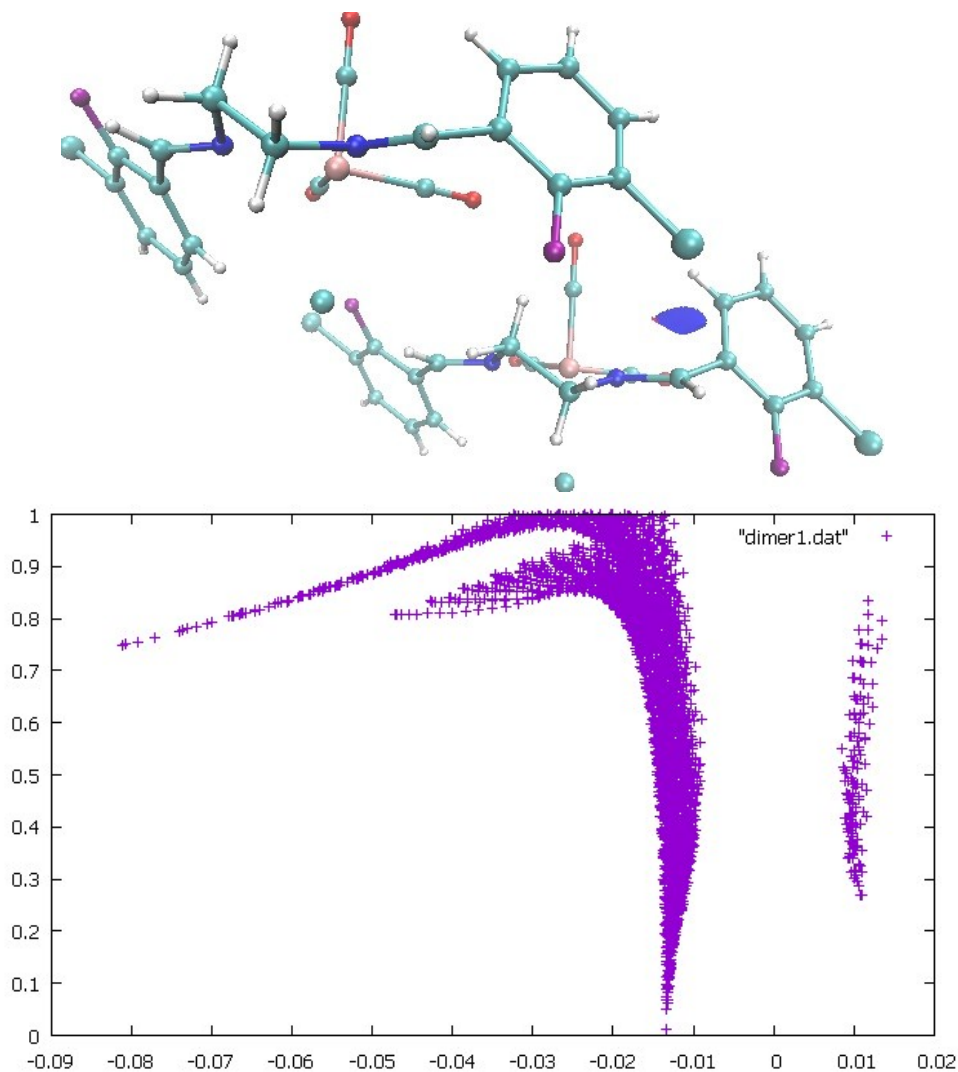


Fig. S35a. Intermolecular **C12...C13** isosurface (top) and its corresponding RDG vs. $\rho \cdot \text{sign}(\lambda_2)$ plot (down) in **C1 (32CIFReBr)**.

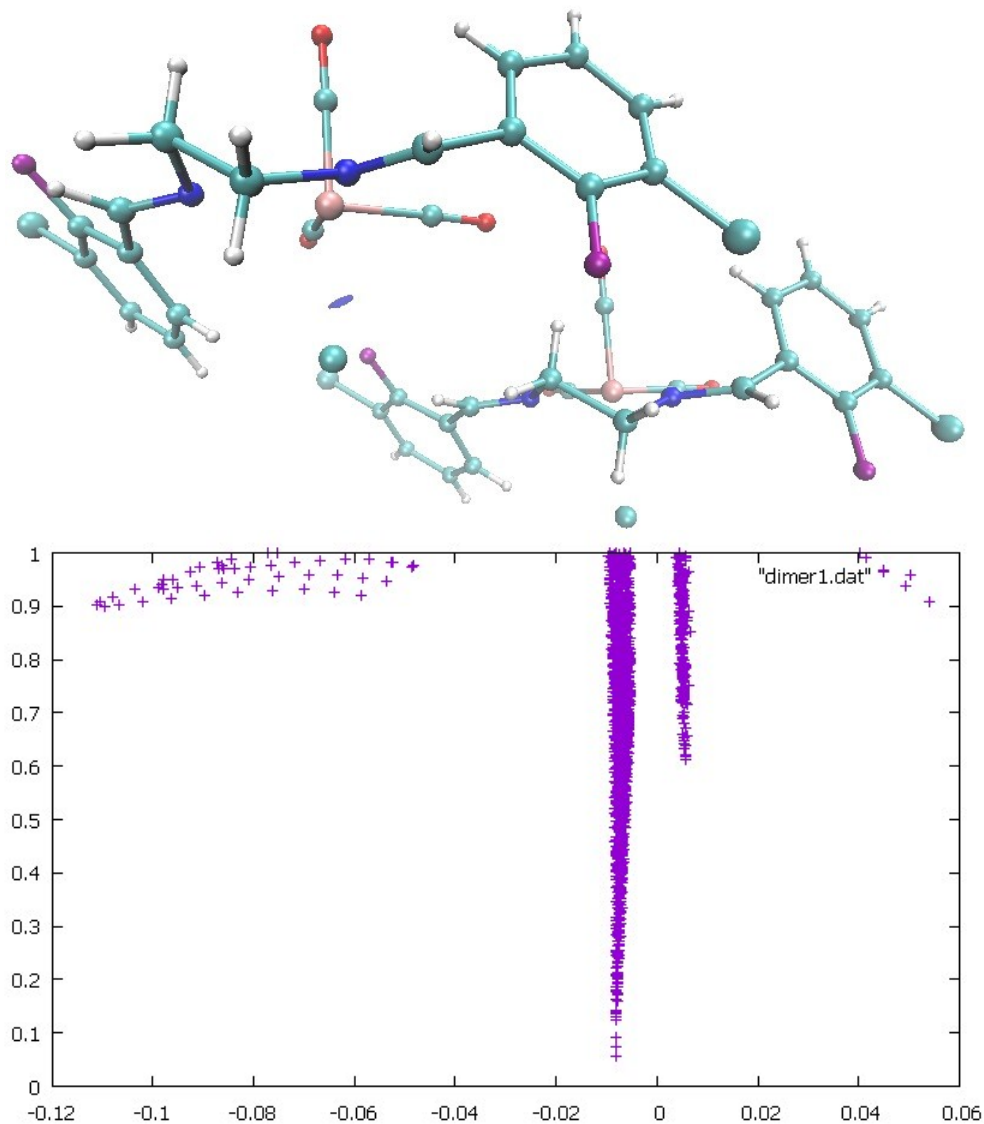


Fig. S35b. Intermolecular F1...O2 isosurface (top) and its corresponding RDG vs. $\rho \cdot \text{sign}(\lambda_2)$ plot (down) in C1 (32ClFReBr).

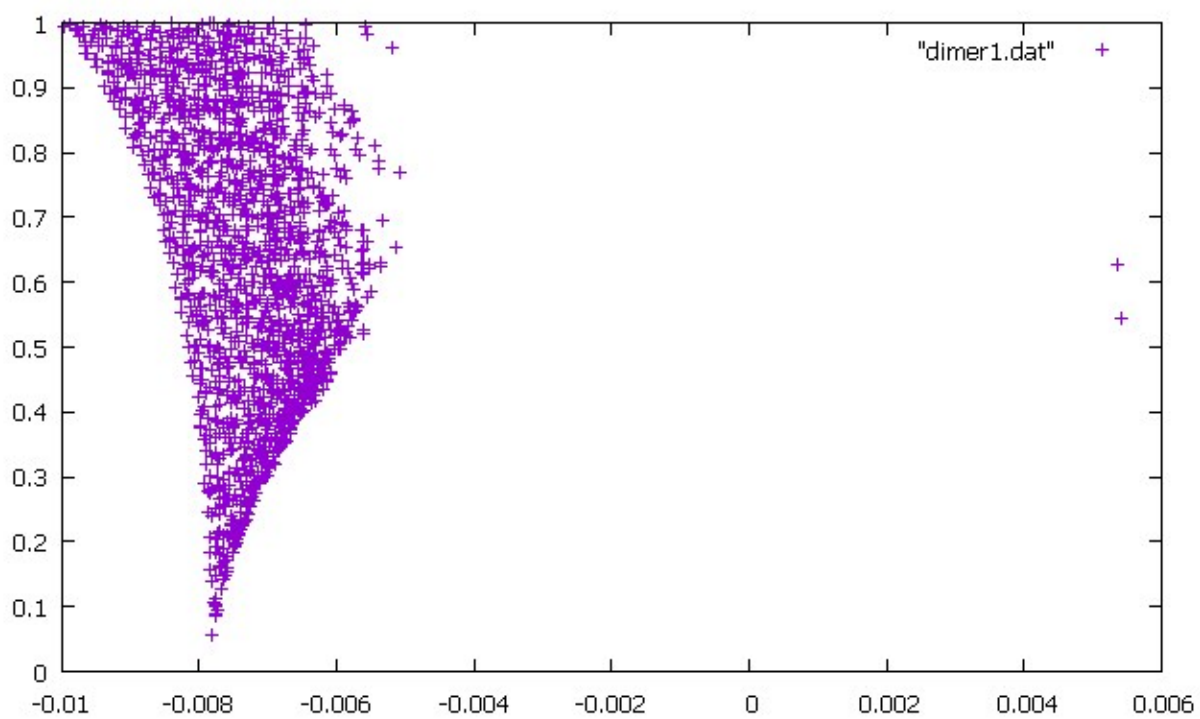
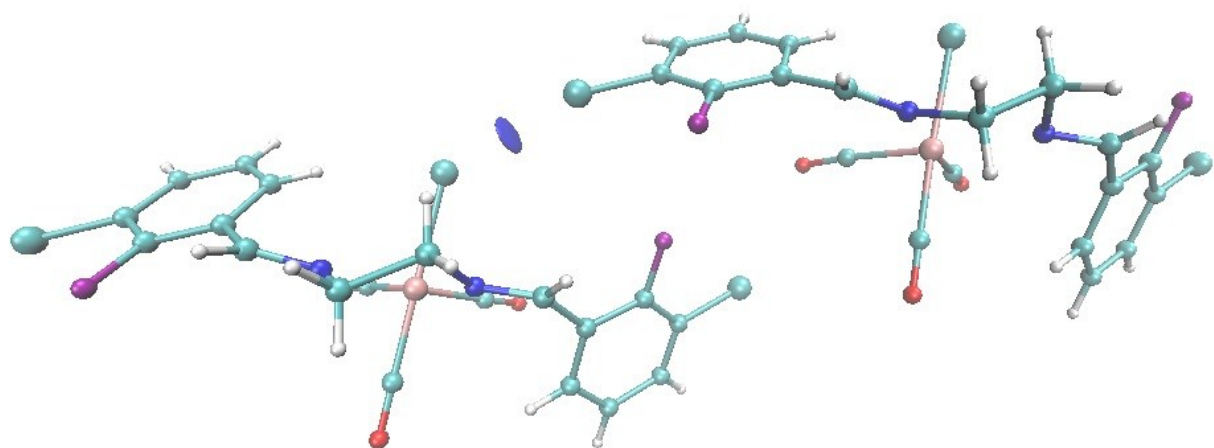


Fig. S35c. Intermolecular **Cl1...Cl3** isosurface (top) and its corresponding RDG vs. $\rho \cdot \text{sign}(\lambda_2)$ plot (down) in **C2 (32CIFReCl)**.

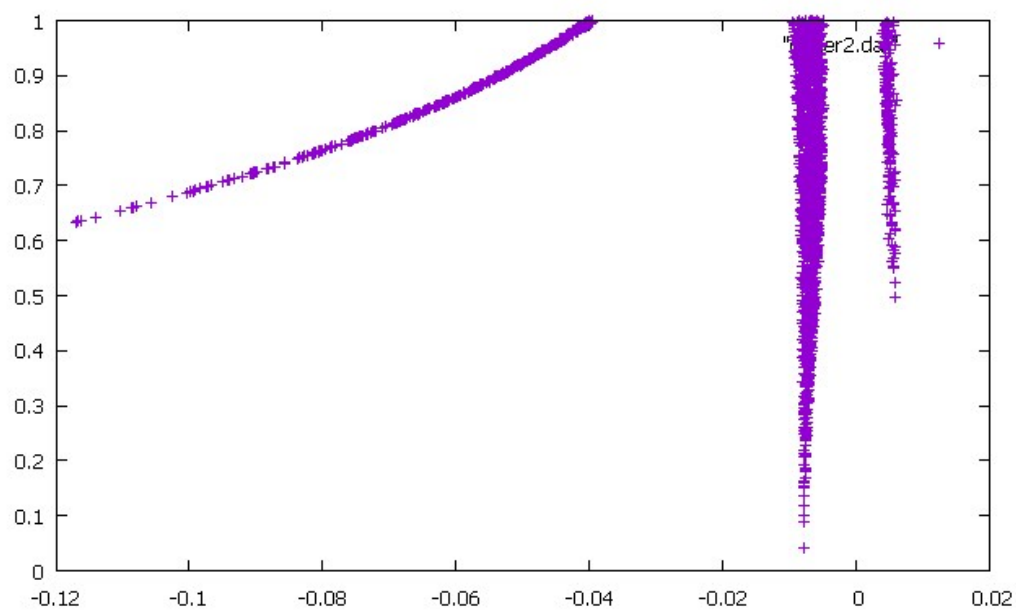
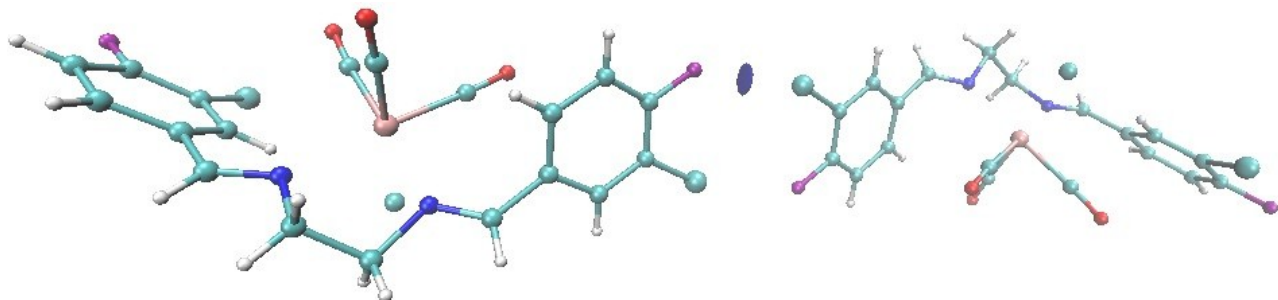


Fig. S35d. Intermolecular Cl1...F1 isosurface (top) and its corresponding RDG vs. $\rho \cdot \text{sign}(\lambda_2)$ plot (down) in C3 (34CIFReBr).

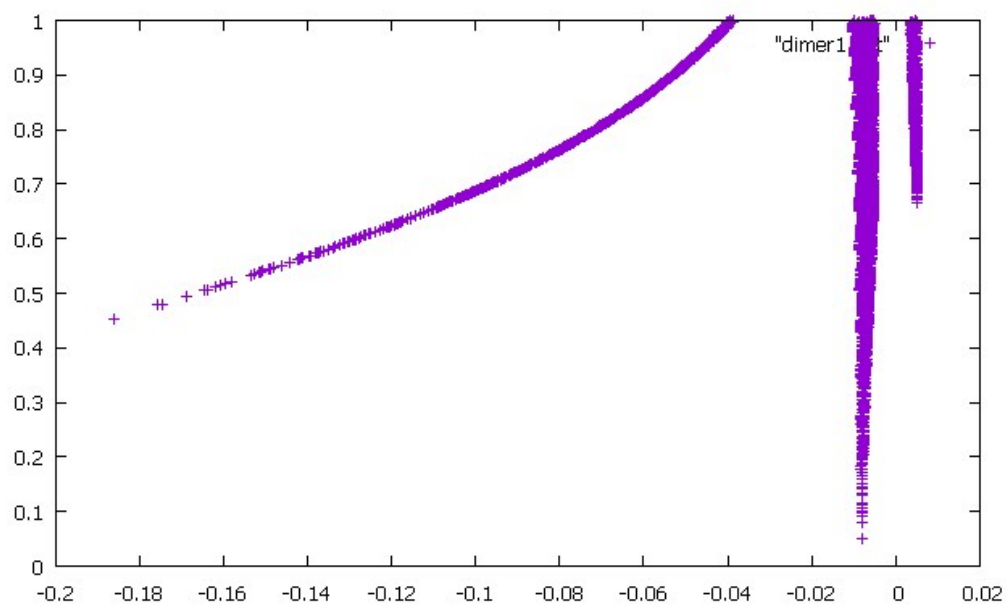
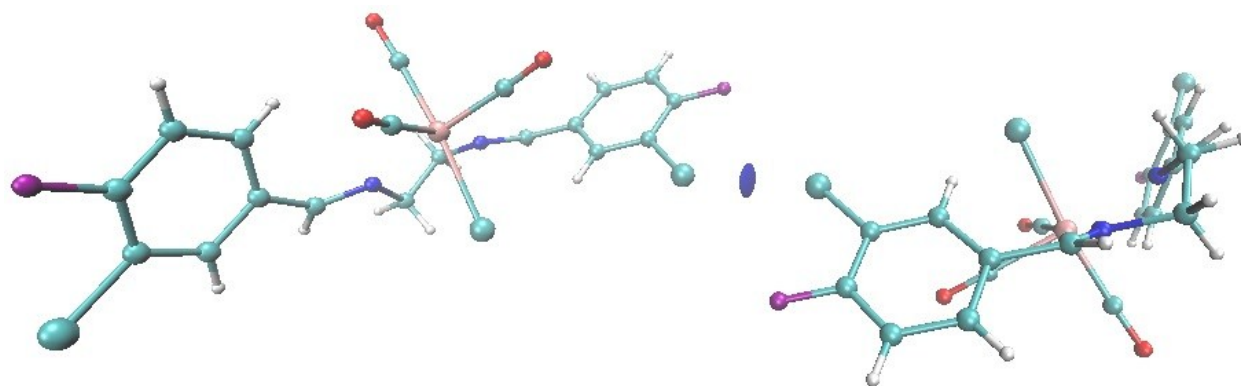


Fig. S35e. Intermolecular Cl2...F2 isosurface (top) and its corresponding RDG vs. $\rho \cdot \text{sign}(\lambda_2)$ plot (down) in C4 (34CIFReCl).

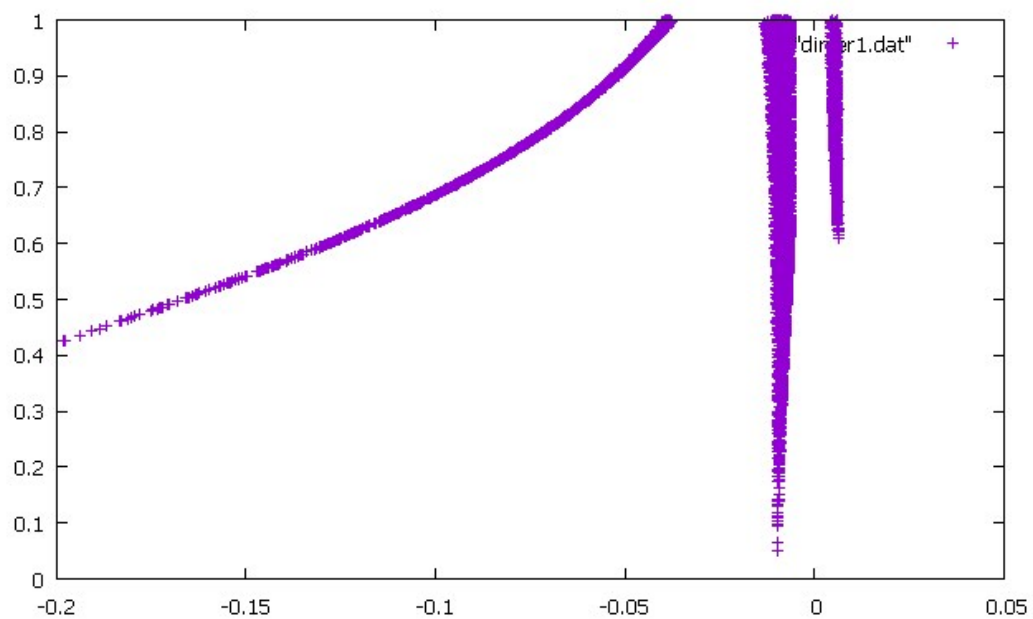
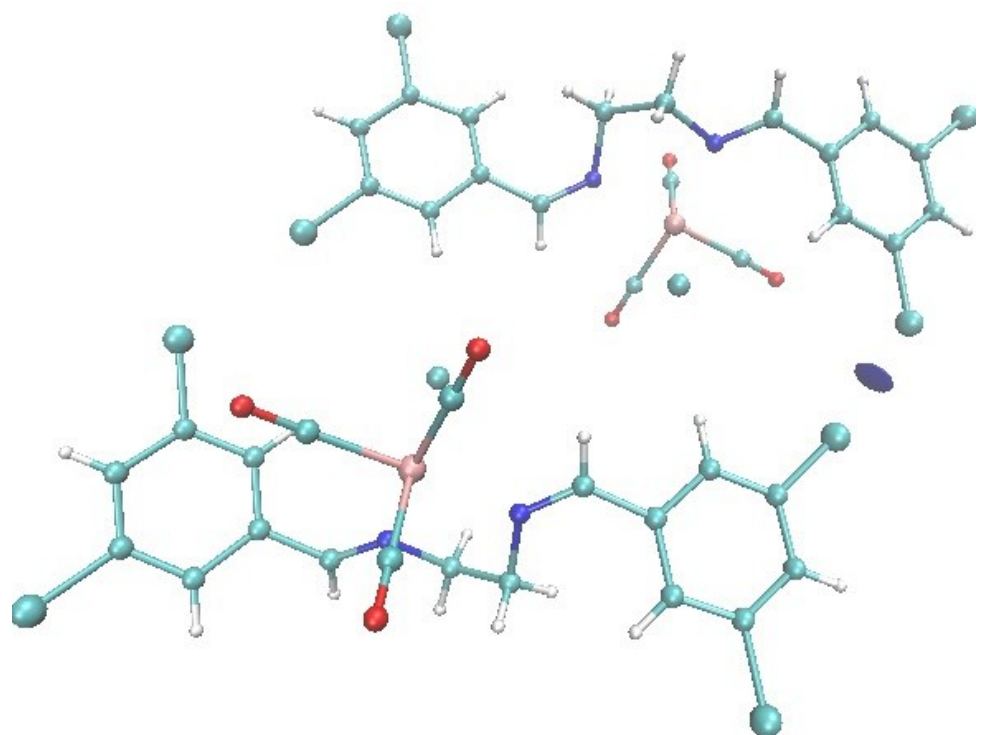


Fig. S35f. Intermolecular C11...Cl3 isosurface (top) and its corresponding RDG vs. $\rho \cdot \text{sign}(\lambda_2)$ plot (down) in C5 (35ClenReBr).

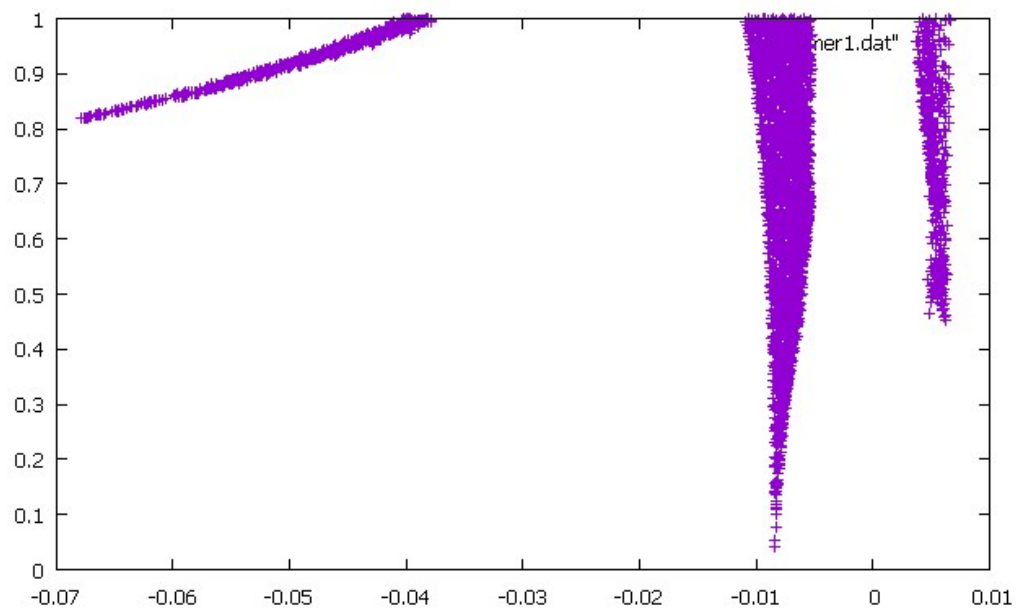
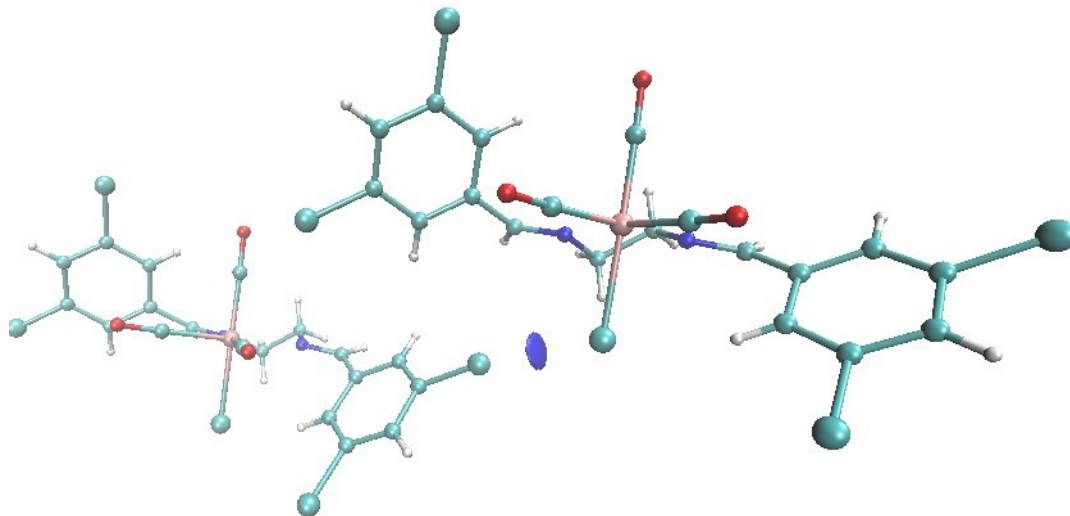


Fig. S35g. Intermolecular Cl1...Cl3 isosurface (top) and its corresponding RDG vs. $\rho^*\text{sign}(\lambda_2)$ plot (down) in C6 (35ClenReCl).

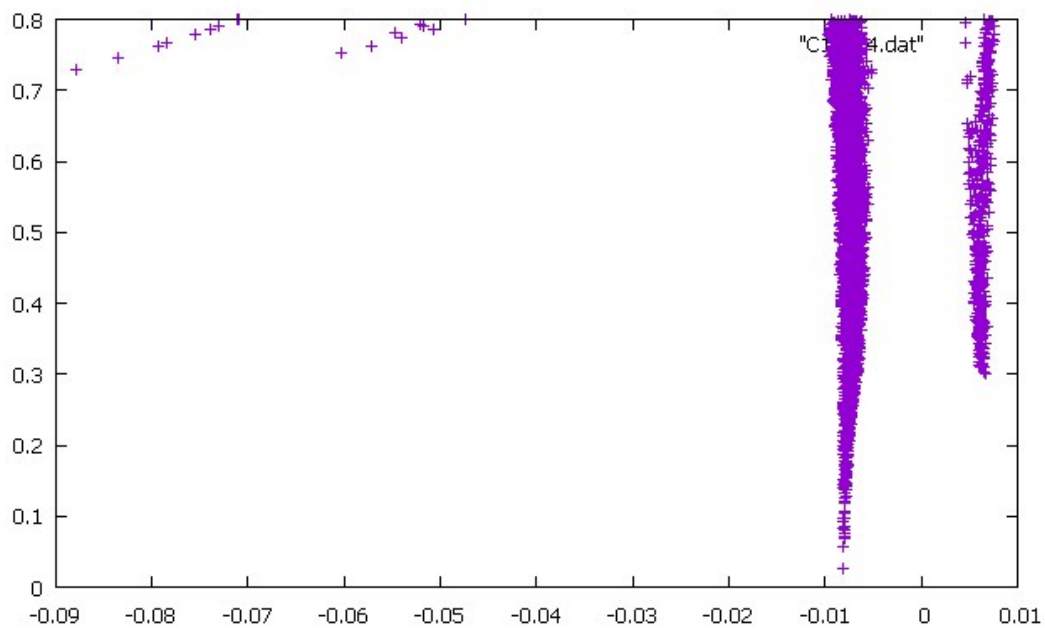
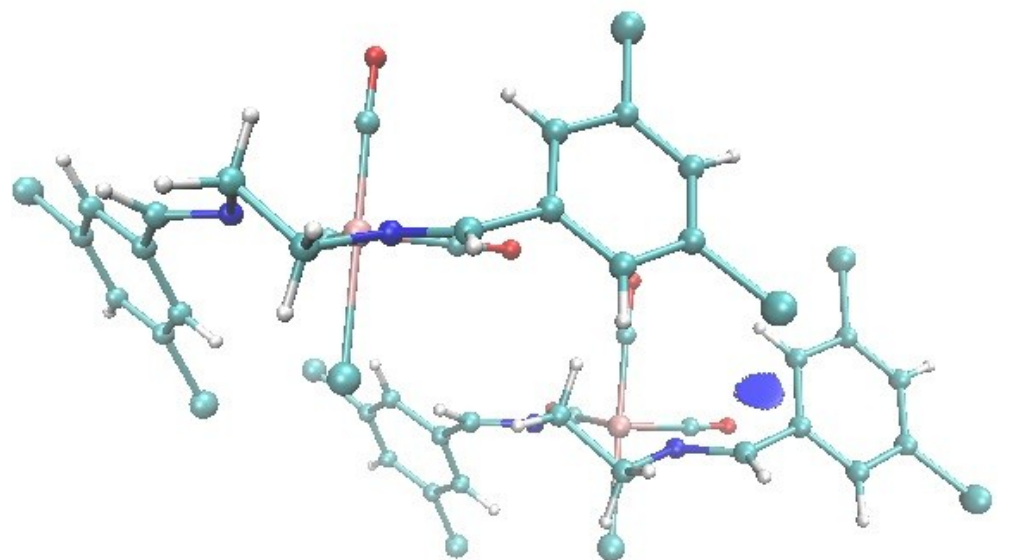


Fig. S35h. Intermolecular **C14...C10** isosurface (top) and its corresponding RDG vs. $\rho \cdot \text{sign}(\lambda_2)$ plot (down) in **C6 (35ClenReCl)**.

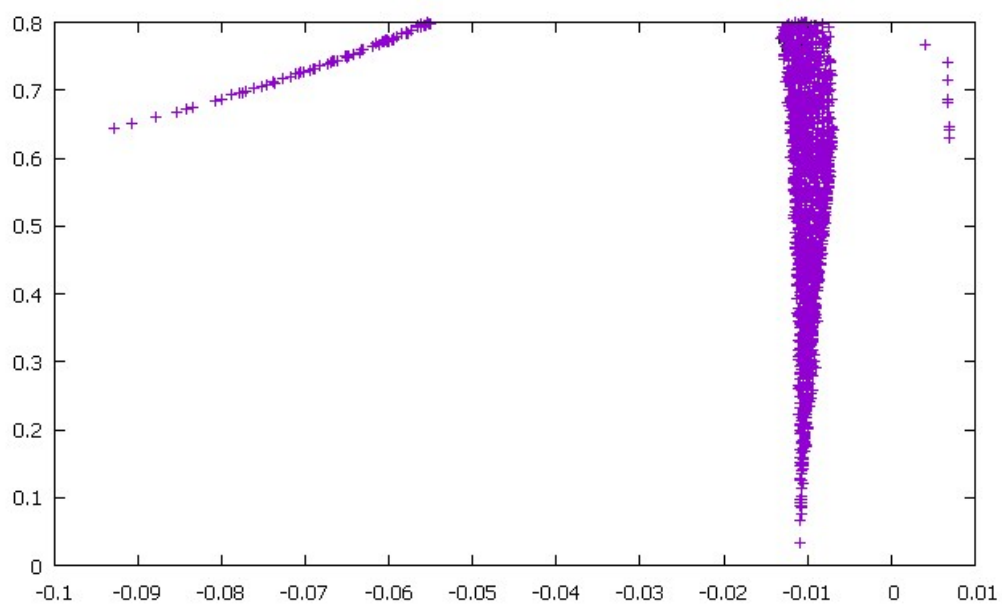
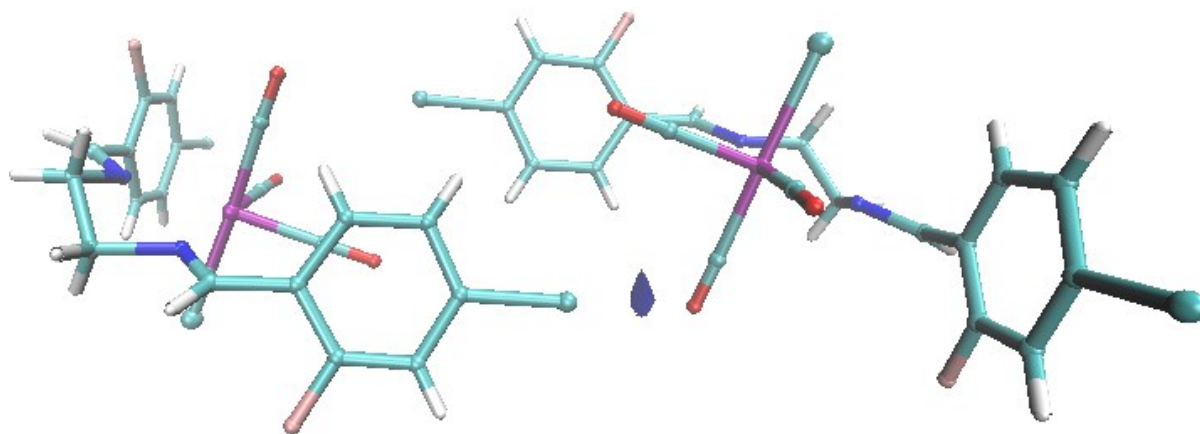


Fig. S35i. Intermolecular **Br1...O3** isosurface (top) and its corresponding RDG vs. $\rho \cdot \text{sign}(\lambda_2)$ plot (down) in **C7 (42BrFenReCl)**.

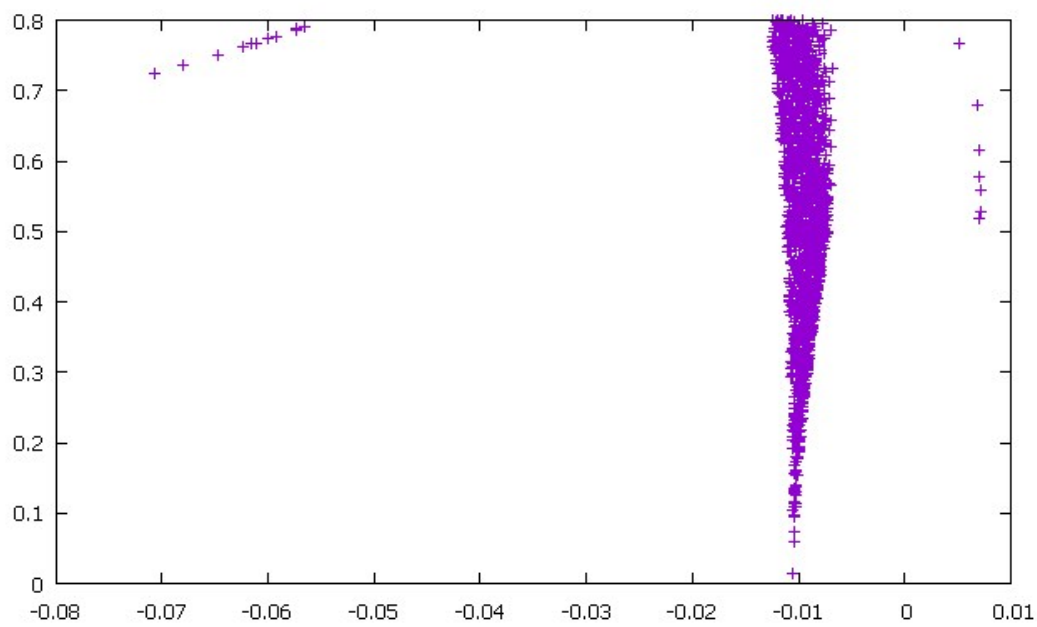
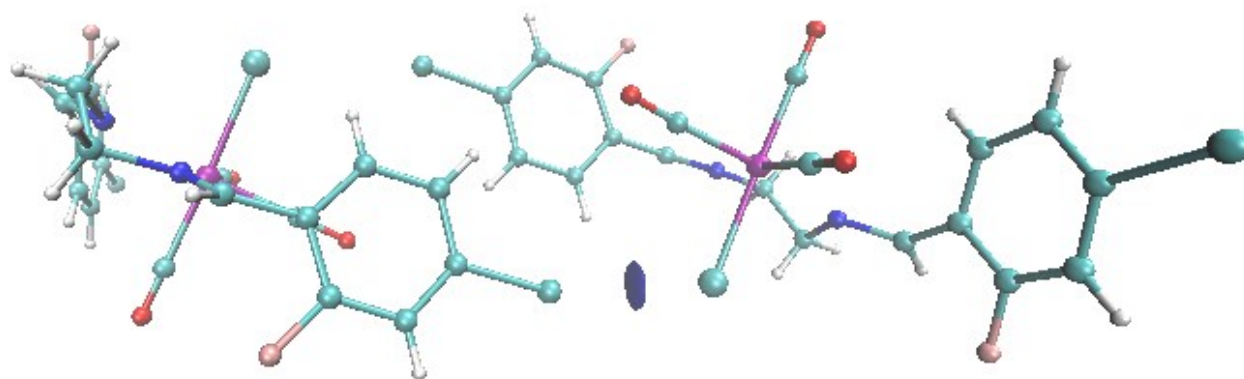


Fig. S35j. Intermolecular **Cl1...Br2** isosurface (top) and its corresponding RDG vs. $\rho^*\text{sign}(\lambda_2)$ plot (down) in **C7 (42BrFenReCl)**.

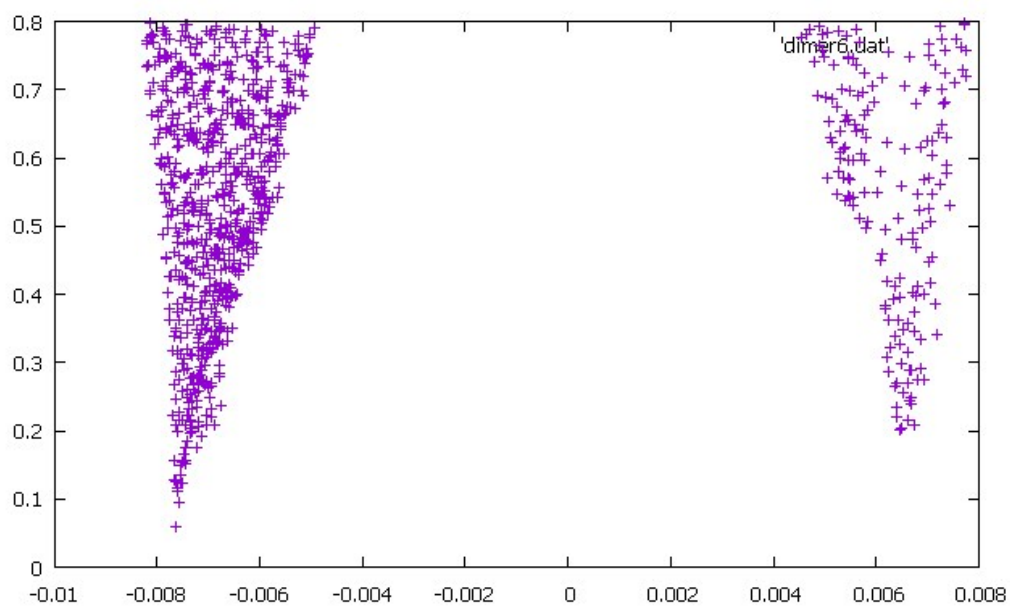
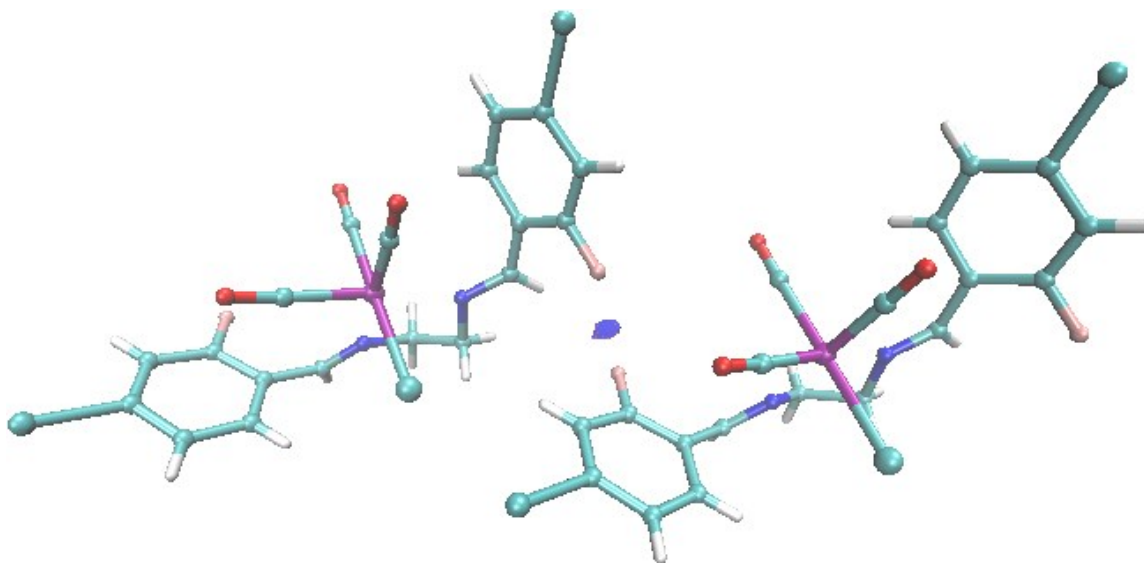


Fig. S35k. Intermolecular $F1 \cdots F2$ isosurface (top) and its corresponding RDG vs. $\rho \cdot \text{sign}(\lambda_2)$ plot (down) in **C7 (42BrFenReCl)**.

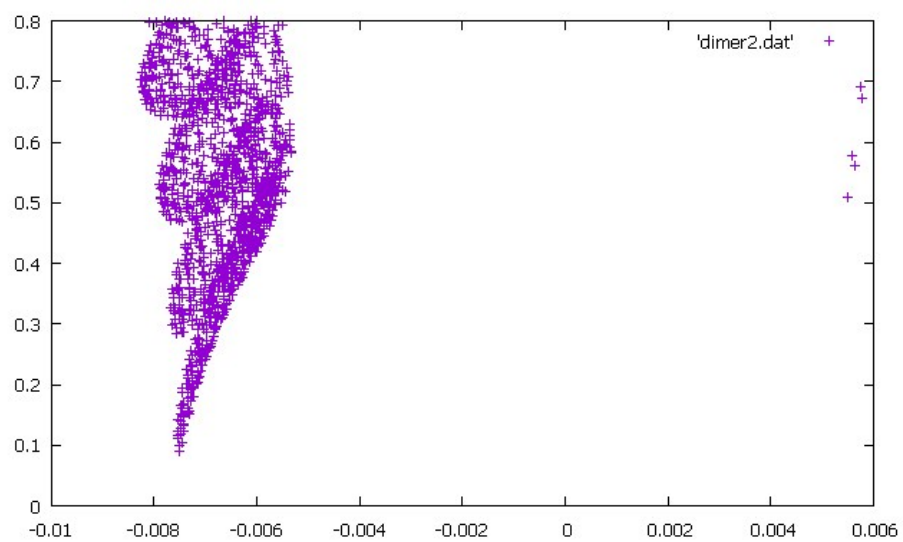
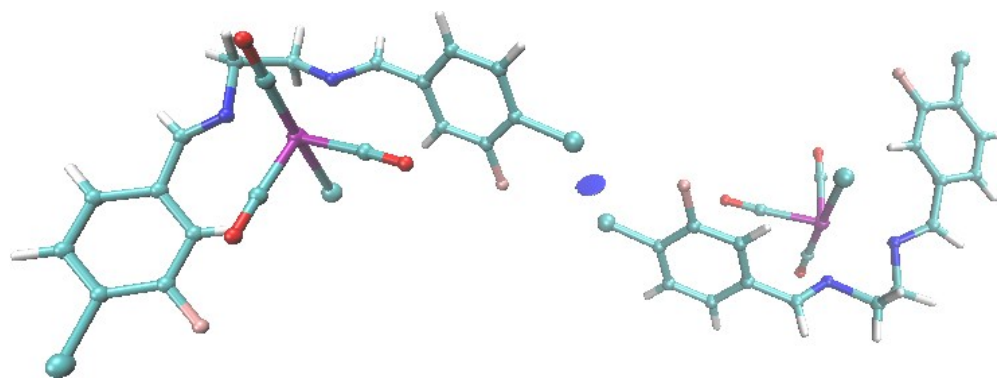


Fig. S35I. Intermolecular C11...C11 isosurface (top) and its corresponding RDG vs. $\rho \cdot \text{sign}(\lambda_2)$ plot (down) in C8 (43ClFenReCl).

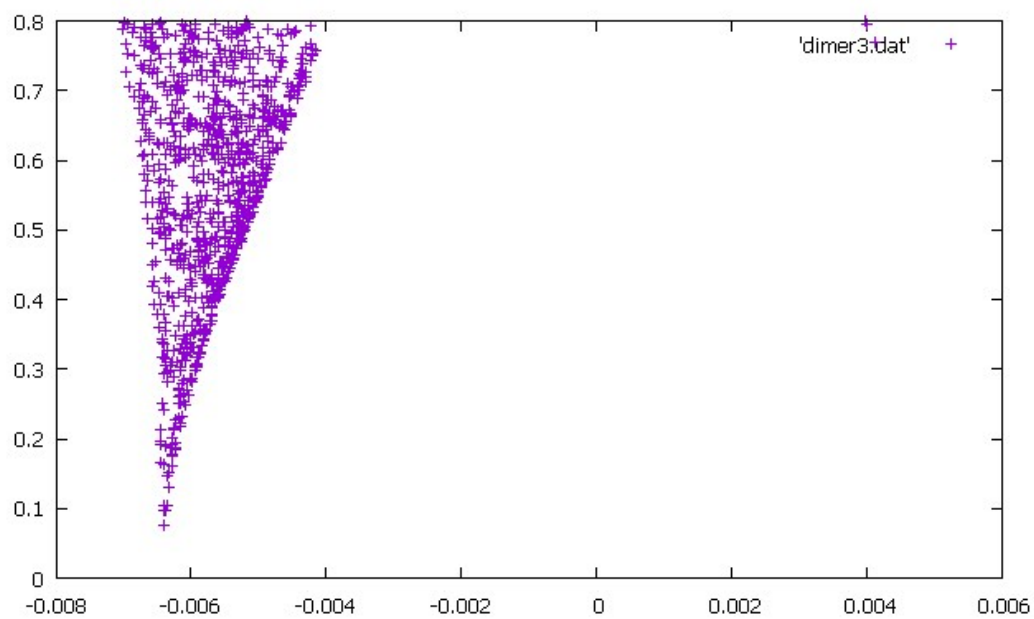
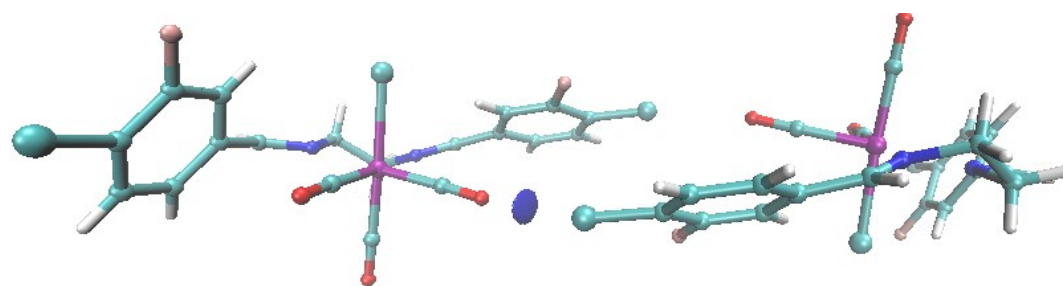


Fig. S35m. Intermolecular Cl2...O2 isosurface (top) and its corresponding RDG vs. $\rho \cdot \text{sign}(\lambda_2)$ plot (down) in **C8 (43ClFenReCl)**.

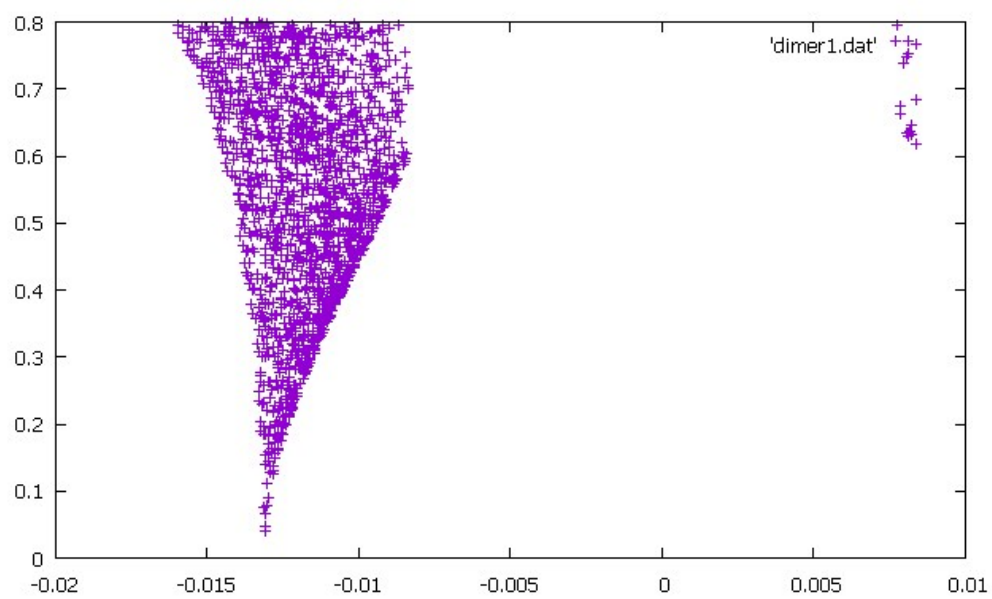
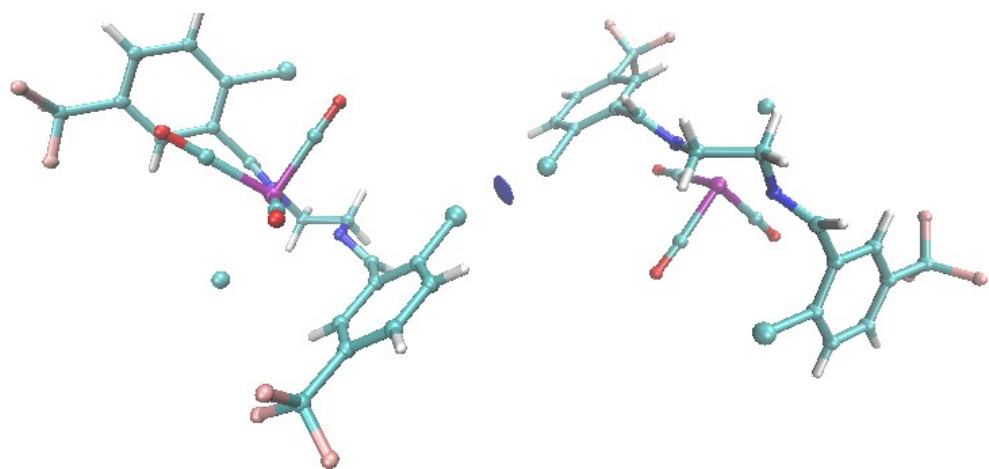


Fig. S35n. Intermolecular Cl1...Cl1 isosurface (top) and its corresponding RDG vs. $\rho \cdot \text{sign}(\lambda_2)$ plot (down) in C9 (ClFenReBr).

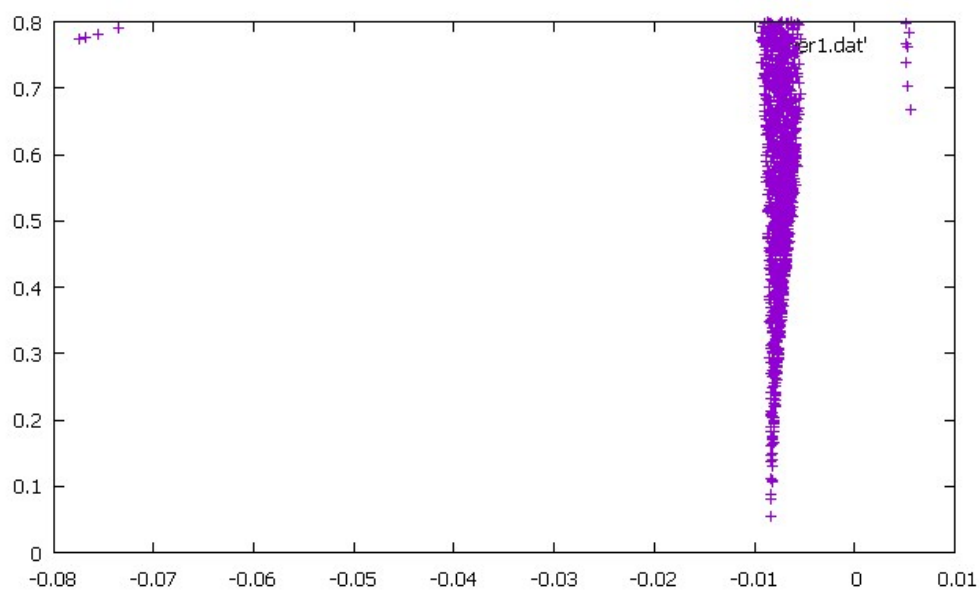
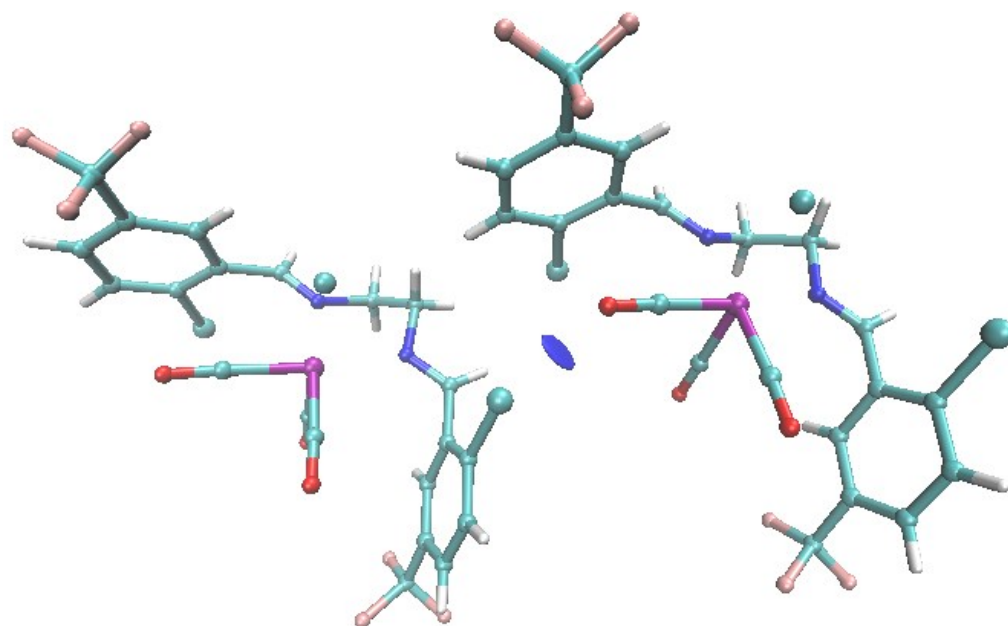


Fig. S35o. Intermolecular **Cl2...O2** isosurface (top) and its corresponding RDG vs. $\rho \cdot \text{sign}(\lambda_2)$ plot (down) in **C10 (ClFenReBr')**.

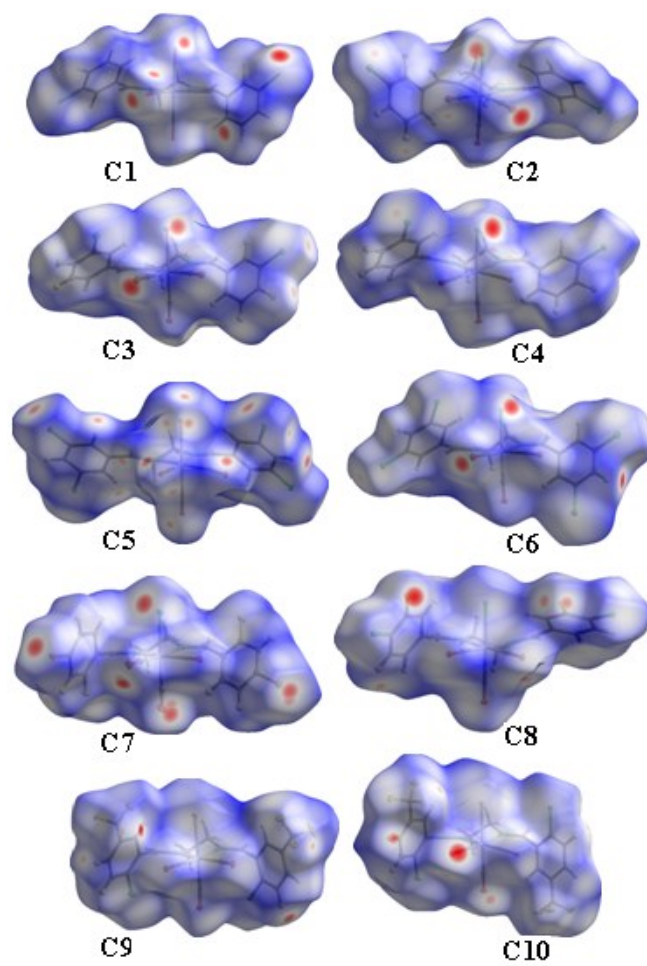


Figure S36. d_{norm} mapped on Hirshfeld surfaces in C1–C10.

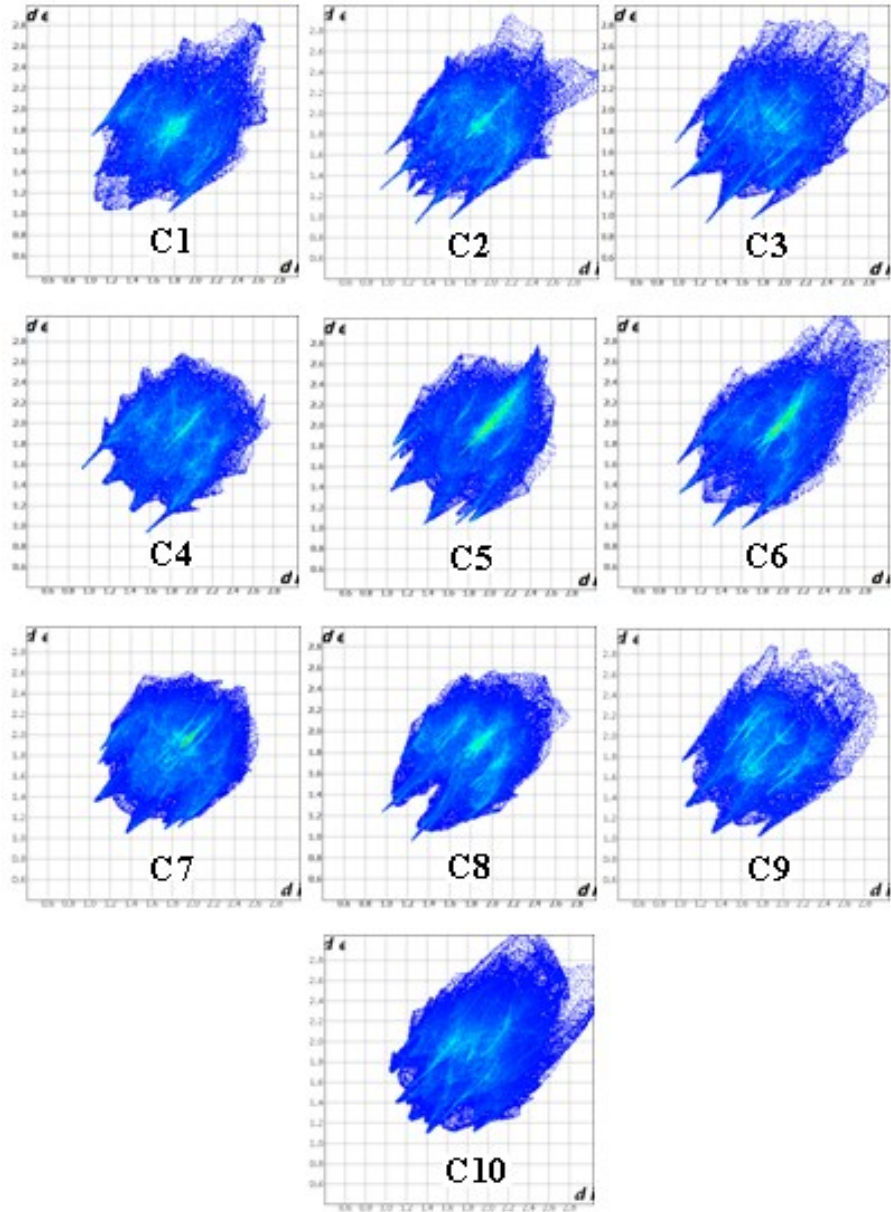


Figure S37. 2D fingerprint plots of observed contacts in C1-C10.